Civil Engineering and Architecture 13(6): 4331-4352, 2025 http://www.hrpub.org
DOI: 10.13189/cea.2025.130616

# Evaluating Urban Surface Materials: Albedo Optimization and Shading for Pedestrian Thermal Comfort in Hot-Arid Environments

**Mayar Ghoniem[1], Amgad Fahmy[1,2], Tarek M. Kamel[1,*]**

[1]Department of Architectural Engineering and Environmental Design, College of Engineering and Technology, Arab Academy for Science, Technology and Maritime Transport, Egypt
[2]Department of Architecture, Effat University, Saudi Arabia

*Received July 31, 2025; Revised October 9, 2025; Accepted October 21, 2025*

***Cite This Paper in the Following Citation Styles***

***(a):*** *[1] Mayar Ghoniem, Amgad Fahmy, Tarek M. Kamel , "Evaluating Urban Surface Materials: Albedo Optimization and Shading for Pedestrian Thermal Comfort in Hot-Arid Environments," Civil Engineering and Architecture, Vol. 13, No. 6, pp. 4331 - 4352, 2025. DOI: 10.13189/cea.2025.130616.*

***(b):*** *Mayar Ghoniem, Amgad Fahmy, Tarek M. Kamel (2025). Evaluating Urban Surface Materials: Albedo Optimization and Shading for Pedestrian Thermal Comfort in Hot-Arid Environments. Civil Engineering and Architecture, 13(6), 4331 - 4352. DOI: 10.13189/cea.2025.130616.*



**Abstract** Enhancing pedestrian thermal comfort in Egypt's hot-arid environments is a growing urban design challenge. This study evaluates the thermal effects of varying surface albedo values (0.12, 0.20, 0.30) in a commercial pedestrian strip in New Cairo, using a hybrid workflow that integrates ENVI-met microclimate simulations, Grasshopper/Ladybug parametric modelling, and field validation. The objective is to assess how reflective material influences surface temperature (Ts), air temperature (Ta), mean radiant temperature (MRT), and Universal Thermal Climate Index (UTCI), and to determine the role of shading in offsetting potential trade-offs. Findings indicate that increasing albedo reduced Ts by up to 7 ℃ and Ta at pedestrian height by 1.5 ℃, confirming the cooling potential of reflective pavements. However, results also showed that higher reflectivity elevated MRT by as much as 6 ℃, which in turn raised UTCI values beyond 46 ℃ in unshaded conditions, placing pedestrians in strong to extreme heat-stress categories. When modular canopy shading was introduced, UTCI declined by 5–6.6 ℃, effectively neutralizing the radiant penalties associated with high albedo and demonstrating that shading interventions are more decisive than material modifications alone. This study contributes to ongoing debates on climate-responsive design in arid cities by highlighting both opportunities and limitations of reflective pavements. While reflective surfaces provide measurable cooling benefits, they must be embedded within layered strategies that include shading and vegetation to ensure pedestrian comfort. Research limitations include the focus on a single urban typology and peak summer conditions, while practical implications emphasize the need for policy frameworks that mandate paired material-shading approaches in public spaces. These findings provide evidence-based guidance for planners and designers seeking to create thermally adaptive, pedestrian-friendly environments in hot-arid contexts.

**Keywords** Outdoor Thermal Comfort, Surface Albedo, Shading, Dark Pavements, Universal Thermal Climate Index (UTCI), Mean Radiant Temperature (MRT), ENVI-met, Ladybug Tools

## 1. Introduction

Urban heat stress is an escalating concern in hot-arid regions, where intense solar exposure, limited vegetation, and thermally absorptive paving materials amplify pedestrian discomfort. This phenomenon, widely documented in the literature, contributes significantly to the Urban Heat Island (UHI) effect and poses heightened risks in already overheated regions [1], [2].

In rapidly expanding cities such as Cairo, commercial and residential projects frequently prioritize aesthetic paving finishes (dark stone, basalt, or asphalt) over climate-sensitive design. These materials typically exhibit low albedo (<0.20), absorbing substantial solar radiation and elevating both surface (Ts) and air temperatures (Ta). While visually appealing, they intensify radiant and conductive heat loads, producing outdoor environments that are visually open but thermally hostile [3], [4].

Urban surfaces (particularly roads, rooftops, and plazas) absorb substantial amounts of solar radiation, contributing to elevated surface and air temperatures in populated areas [5]. The combination of thermal mass, low albedo materials, and sparse shading accelerates localized heat buildup and reduces overall outdoor livability [6], [7]. In response, thermally adaptive design approaches are being increasingly prioritized to enhance urban resilience, especially as walkability and outdoor recreational use become core planning objectives in modern city design.

Despite these developments, thermal comfort is still frequently overlooked in the design of public spaces within many Egyptian urban projects [2], [3], [6]. Wide pedestrian promenades, low-rise commercial buildings, and decorative yet heat-retaining paving materials are often favored over climate-sensitive features such as shade structures, optimal orientation, or reflective surfaces [2], [4]. As a result, many urban spaces in Egypt remain visually open but thermally unwelcoming, with minimal interventions to reduce radiant and conductive heat stress [2]. This imbalance calls for integrated environmental design strategies that align visual, spatial, and thermal goals to promote healthier and more comfortable outdoor environments.

This study aims to evaluate the role of material reflectivity (specifically surface albedo) in shaping microclimatic conditions within one such exposed setting, a commercial pedestrian strip in New Cairo. By simulating and validating different albedo configurations under fixed morphological conditions, the research seeks to quantify their impact on $T_s$, $T_a$, and thermal comfort indices at the pedestrian level [4], [6]. The findings contribute to broader efforts to optimize material selection as a passive cooling strategy in arid cities and offer design guidance for future urban developments in Egypt and similar climatic contexts [3], [6].

Despite increasing awareness of urban heat mitigation strategies, the market-driven push for visually luxurious pavements continues to promote the use of dark, heat-retaining materials in pedestrian zones [2]. This paradox highlights the need for evidence-based evaluations of how surface reflectivity, independent of aesthetic trends, influences thermal comfort [6]. Heat exposure in these outdoor spaces not only affects comfort but also poses increasing public health risks, particularly for vulnerable populations during peak summer periods [1]. A growing body of reviews consolidates the urban heat mitigation toolbox (cool materials, shade/vegetation, and morphology) while cautioning that benefits are context-dependent and must be evaluated at the pedestrian scale [8].

To address this, the study employs validated microclimate simulations using ENVI-met 5.7.1 and Grasshopper workflows to assess the thermal impact of surface reflectivity [9]. The combination of ENVI-met and Grasshopper was selected for its capacity to simulate detailed microclimatic variables while allowing for controlled parametric adjustments in surface material reflectivity and configuration [6], [9]. These findings are intended to inform future planning guidelines and urban material selection protocols in Egypt's emerging cities, supporting the design of thermally responsive pedestrian infrastructure [6].

However, simulation-based, context-specific studies isolating the impact of surface albedo on thermal comfort in Egypt's new commercial developments remain scarce, with only limited regional studies addressing this gap [2], [6], [7].

### 1.1. The Role of Surface Albedo

Surface albedo (the ratio of reflected to incident shortwave radiation) is a first-order control on how much heat urban surfaces absorb and later re-emit to pedestrians. Parametric microclimate work shows that tuning both ground and wall reflectivity can measurably reshape pedestrian-level conditions by altering shortwave loads, longwave exchange, and the balance between convective and radiative fluxes [9]. In hot-arid settings such as Cairo, where solar loading is high and sky view is often unobstructed, raising pavement reflectivity reduces absorbed shortwave energy and suppresses daytime surface temperatures (Ts); near-surface air temperature (Ta) typically follows in the same direction, but with smaller magnitudes than the surface response [10].

Albedo does not operate in isolation from shade. Field and simulation studies on shading devices show that geometric shade is the dominant lever on the radiant environment and sets the ceiling for comfort gains at pedestrian height; without shade, making the ground more reflective can shift part of the heat burden from the surface to the body via increased shortwave reflections [11]. At the level of aggregated evidence, a systematic review and meta-analysis reports statistically significant decreases in midday Ts with increasing pavement albedo, generally in the low-single-digit ℃ range for modest albedo increments and larger reductions when shifting from dark asphalt baselines to high-reflectance finishes [12]. A complementary state-of-the-art review catalogs practical cool-pavement technologies (coatings, light aggregates, modified binders) and documents double-digit ℃ midday Ts reductions for reflective asphalt coatings ($\alpha \approx 0.46–0.57$) compared with conventional asphalt, while emphasizing application context, durability, and maintenance as determinants of sustained performance [13].

Critically, reflective materials are not thermally neutral for pedestrians in open sites. Mediterranean plaza observations show that high-albedo surfaces can lower Ts by several degrees yet raise mean radiant temperature (MRT) (and consequently UTCI) in unshaded conditions due to intensified shortwave reflections at the body level [14]. In Cairo, spatial analysis of thermal fields further demonstrates anisotropic responses across the street fabric, so the net benefit of higher reflectivity depends on exposure, enclosure, and adjacent façade/material properties [15]. Consistent with this, studies that combine cool pavements with trees or other shade report the most robust comfort gains: site-scale Ta decreases accompanied by substantial MRT relief beneath canopy, indicating that reflective materials perform best when embedded within layered, shade-providing strategies [16].

For local relevance, Cairo-grounded evidence using a hybrid ENVI-met/parametric workflow with field checks shows that raising pavement albedo from a dark baseline (~0.12) toward reflective finishes produced Ts reductions up to ≈12.9 °C and Ta reductions up to ≈2.0 °C during summer daytime periods; the same work confirms radiant penalties in unshaded areas, reinforcing the need to pair albedo optimization with geometric shade in exposed strips [6], [11], [16].

### 1.2. Outdoor Thermal Comfort Indices

Outdoor thermal comfort (OTC) represents a multifactorial response to the surrounding microclimate, shaped not only by $T_a$ but also by solar radiation, wind velocity, humidity, and surface characteristics. To capture these complex interactions, composite indices are preferred over single-variable metrics. Among these, the Universal Thermal Climate Index (UTCI) and Mean Radiant Temperature (MRT) are the most widely used in hot-arid urban climatology [17]. Synthesis papers likewise recommend composite, radiation-sensitive indices (UTCI, PET) over single-variable metrics when evaluating open, sun-exposed urban realms, due to the dominant role of shortwave and longwave exchanges in perceived heat stress [8].

UTCI is based on a multi-node thermoregulatory model and integrates dynamic meteorological inputs such as Ta, wind speed, humidity, and short- and longwave radiation [18]. Its high sensitivity to solar radiation makes it especially suitable for outdoor pedestrian studies in sun-exposed environments like those found in Egypt and the broader MENA region, where vegetation also plays a role in mitigating surface heat [19], [20], [21]. MRT, while not a stand-alone index, remains a critical parameter in microclimatic modeling and is directly linked to radiant heat load and thermal stress; validated MRT simulations in hot-arid contexts confirm its central role [17]. MRT, while not a stand-alone index, remains a critical parameter in microclimatic modelling and is directly linked to radiant heat load and thermal stress; validated MRT simulations and microclimate workflow verification in hot-arid contexts confirm its central role [17], [22].

The selected research spans simulation, hybrid, and field-based methodologies and demonstrates the reported thermal improvements from interventions like surface albedo modification and urban form adjustment [19], [23].

Recent studies across hot-arid regions have highlighted the importance of validating outdoor thermal comfort modelling through ENVI-met simulations supported by field measurements [19], [24]. Simulation-based studies on reflective pavement strategies recorded meaningful UTCI improvements under arid conditions through albedo optimization and scenario testing [25]. Similarly, comparative canyon-scale analyses confirmed MRT reductions following material albedo enhancement and vegetation interventions [26].

Field and hybrid validation studies further demonstrate that reflective pavements and passive measures can significantly reduce heat exposure in hot-arid cities [23], [24]. In desert climate field tests, cool pavement applications demonstrated surface temperature reductions of up to ~12 ℃ and air temperature decreases of around 1-2 ℃ after applying light-colored materials [23]. Yet, as shown in Egyptian ENVI-met case studies, reductions in Ts did not consistently align with improved comfort: elevated shortwave reflections increased MRT and UTCI in unshaded zones [19]. These outcomes reinforce the need to assess OTC using composite indices, rather than relying solely on Ts [19], [26].

This study adopts UTCI as the principal metric due to its ability to evaluate thermal exposure in outdoor settings holistically [17], [18]. Its consideration of wind, humidity, and radiation, alongside human physiology, makes it more appropriate than indices like PMV, which lack sensitivity to radiant fluctuations [18].

Ultimately, as demonstrated across albedo-focused case studies [6], [14], [16], [25], the impact of surface reflectivity on UTCI and MRT is highly context-specific, underscoring the need for validated modelling frameworks [6], [19], [24]. The variability in outcomes across Cairo and Mediterranean contexts highlights the necessity of calibrated, site-specific modelling and reinforces the importance of complementary design measures, such as shading structures, to mitigate MRT increases associated with reflective pavements [14], [16], [25].

While albedo optimization can reduce Ts and Ta, its reflective properties may elevate MRT and UTCI in unshaded conditions. This confirms the need to pair reflective pavements with shading and vegetative measures to ensure pedestrian comfort [6], [16], [25], [26].

The scope of this study was limited to a single commercial strip typology in New Cairo under controlled boundary conditions. While this allowed for the isolation of albedo effects, it also constrains the generalizability of findings to other urban morphologies or mixed-use settings. Future work should therefore incorporate diverse urban forms, vegetation strategies, and long-term monitoring to capture the interactive dynamics between surface reflectivity, shading, and morphology [3], [19], [20], [21].

Ultimately, the findings contribute to evidence-based urban design guidance by clarifying both the benefits and limitations of albedo-based cooling strategies. Integrating reflective materials with morphological and vegetative design offers the most resilient path toward thermally adaptive, pedestrian-friendly public spaces in hot-arid contexts [6], [16], [24].

The novelty of this study lies in its hybrid validation approach, combining ENVI-met and Grasshopper simulations with field measurements to isolate the thermal impacts of albedo under hot-arid conditions. By explicitly quantifying both convective (Ts, Ta) and radiative (MRT, UTCI) effects, and testing shading integration, this work provides new evidence for how reflective pavements should be deployed in Egypt's emerging urban districts.

## 2. Methodology

This study employs a hybrid research methodology integrating empirical fieldwork, parametric modeling, and validated microscale simulation to assess the impact of surface albedo on pedestrian thermal comfort in a hot-arid urban context. The case study focuses on a commercial strip within a residential compound in New Cairo, representative of the region's built morphology and climate.

The workflow consists of three interconnected phases: (1) field data acquisition and site documentation, (2) digital environmental modeling, and (3) scenario-based simulation and thermal analysis. This workflow, shown in Figure 1, ensures a robust and controlled investigation of surface reflectivity as a passive cooling strategy [16].

Field measurements were conducted during peak summer conditions, capturing $T_a$, $T_s$, globe temperature, relative humidity, and wind speed at five key time intervals throughout the day [27], [28]. These parameters were selected for their relevance to thermal comfort modeling and their role in validating and calibrating the simulation models. Mean Radiant Temperature (MRT) was derived from globe temperature using ISO 7726 standards [29], and Universal Thermal Climate Index (UTCI) values were calculated through validated post-processing techniques [22]. Building on these standardized measurements, recent methodological advances in Egypt have introduced a comprehensive workflow that integrates ENVI-met outputs with parametric modelling environments, ensuring high-fidelity thermal comfort evaluation in hot-arid conditions [21]. In parallel, durability remains a key methodological concern, as field studies in arid climates show that the long-term thermal performance of reflective pavements declines due to albedo degradation from soiling and weathering [4], with additional evidence demonstrating that pavement radiative and thermal properties govern both short-term cooling efficiency and long-term durability of reflective strategies [30]. Complementary methodological studies further confirm the need for such durability considerations in thermal comfort workflows [31].

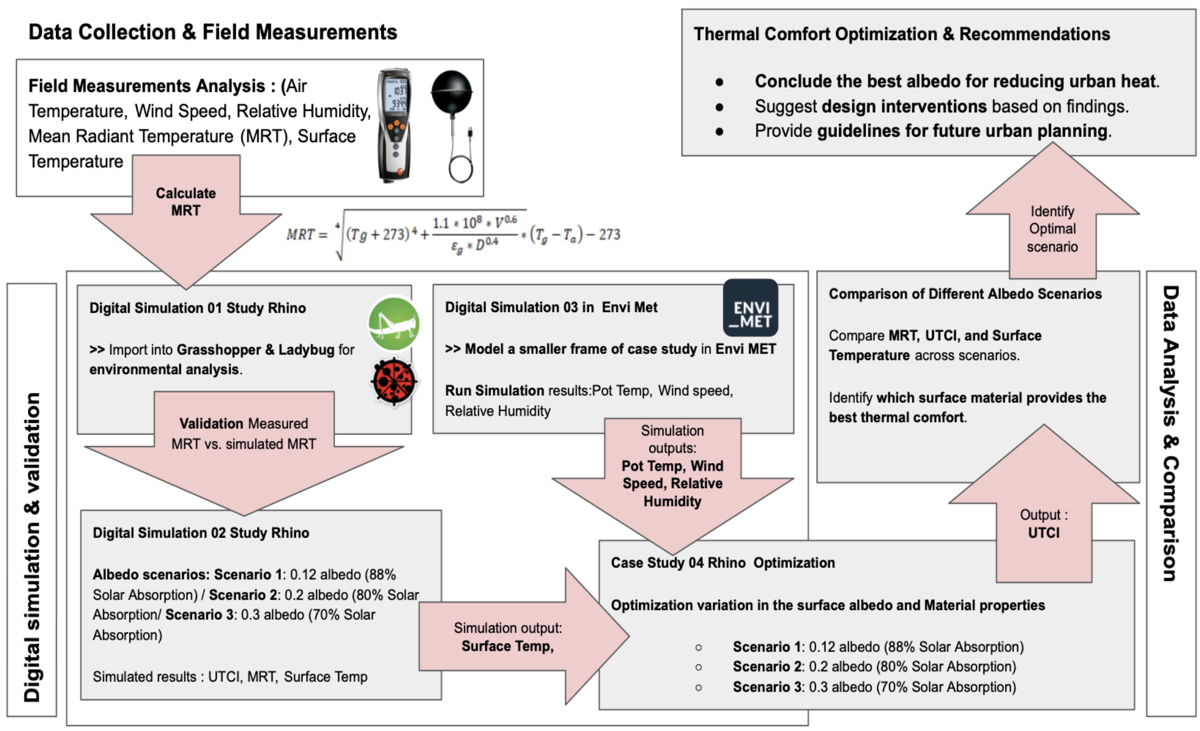


**Figure 1.** Methodological workflow depicting stages of field data collection, environmental modeling, and index computation in the commercial strip case study

A detailed 3D model of the site was constructed using Rhinoceros 3D and Grasshopper, enabling precise spatial representation and parametric manipulation of surface reflectivity. Simultaneously, a high-resolution ENVI-met 5.7.1 model was developed to simulate $T_a$, $T_s$, wind velocity, and relative humidity (RH) within a $50 \times 50$ m subsection of the site [21], [31]. ENVI-met' radiation balance and MRT outputs have been evaluated against field data [27], and the model is widely applied in urban heat studies [32].

To isolate the thermal effect of albedo, all non-material parameters (vegetation, geometry, and weather inputs) were held constant across three scenarios. Validation was conducted for the base case scenario using both Grasshopper and ENVI-met outputs, with simulated MRT and $T_a$ values compared against field measurements to ensure model reliability before testing alternative configurations [22], [31], [33], [34].

Importantly, UTCI and MRT were not simulated directly in ENVI-met; instead, comfort-related insights were computed through calibrated outputs [9]. Recent street-canyon simulations demonstrated the reliability of this approach in assessing albedo-vegetation scenarios [26]. By isolating surface reflectivity as the sole manipulated variable, the study offers evidence-based guidance for integrating albedo optimization into thermally responsive design strategies for outdoor spaces in arid regions [6].

### 2.1. Analytical Framework

This study employed a workflow simulation and comparison methodology to evaluate the thermal impact of surface albedo on pedestrian outdoor comfort in a hot-arid urban environment. The analysis emphasized isolating the independent variable (surface reflectivity) while maintaining uniform urban morphology and vegetative elements across scenarios [9]. Simulations and computations generated outputs for $T_a$, $T_s$, mean radiant temperature (MRT), and the Universal Thermal Climate Index (UTCI) [22]. The workflow followed recent methodological practices applied in arid climate zones for outdoor thermal analysis [6], [21], [31].

The selected urban segment comprised a hardscape pedestrian commercial strip typical of emerging districts in New Cairo. Its exposed layout, with minimal vegetative or shading interventions, made it suitable for examining the thermal implications of albedo variations under peak summer conditions [19]. The simplified geometry and uniform land use minimized extraneous thermal influences. Systematic reviews of thermal comfort modelling similarly highlight the use of morphological simplifications in parametric frameworks to enhance variable isolation and computational efficiency [35].

A custom parametric script was developed in Grasshopper (Rhino 3D), integrating components from the Ladybug tools to simulate and analyze outdoor thermal conditions under different albedo scenarios. The workflow was structured to input environmental parameters (such as $T_a$, relative humidity, and wind speed) alongside modeled urban geometry and material properties [6].

The script employed the Human to Sky Relationship component to evaluate sky exposure and body exposure at the pedestrian level. These outputs were used as inputs for the Outdoor Solar MRT module, which calculates Mean Radiant Temperature (MRT) by accounting for both shortwave and longwave radiation based on surface reflectivity and solar position.

Mean Radiant Temperature (MRT) was calculated using ISO 7726 [29]:

$$T_{mrt} = \left[\left(T_g + 273.15\right)^4 + \ \backslash frac\ \{\ 1.1 \times 10^8,\ V^{\{0.6\}}\}\ \{\varepsilon, D^{\{0.4\}}\},\ \left(T_g - T_a\right)\right]^{\frac{\{1\}}{\{4\}}} - 273.15$$

(Equation 3.1: MRT)

Where $Tg$ is globe temperature (℃), $Ta$ air temperature (℃), $v$ wind speed (m/s), $\varepsilon$ emissivity, and $D$ globe diameter (m).

The Universal Thermal Climate Index (UTCI) was derived from the validated UTCI-Fiala model, integrating Ta, MRT, wind speed, and RH according to ISO standards.

To compute Universal Thermal Climate Index (UTCI), the derived MRT values were fed into the UTCI Comfort component, in combination with climatic data. $T_s$ simulation was handled through an earlier version of Ladybug due to its retained compatibility with surface-based radiation workflows.

The model allowed for parametric adjustment of albedo values across urban surfaces, supporting iterative thermal analysis while keeping all other variables (geometry, vegetation, and atmospheric inputs) constant. This modular script enabled scenario testing for three reflectivity levels (0.12, 0.20, and 0.30) to isolate the thermal effects of surface albedo changes.

Three surface material scenarios were defined by solar absorptance values of 0.88, 0.80, and 0.70, translating to albedo values of 0.12, 0.20, and 0.30, respectively. Each case retained identical spatial geometry, vegetation distribution, and boundary meteorological data, ensuring that surface reflectivity was the sole manipulated variable [9]. By reflecting incident shortwave radiation, high-albedo surfaces reduce absorbed solar energy, which in turn lowers $T_s$. However, this repulsion effect can redirect shortwave radiation toward pedestrians, increasing MRT; field and plaza studies also show spatial variability of these exposures across open sites and street fabrics [14], [15].

Environmental variables were simulated at five-time intervals (09:00, 11:00, 13:00, 15:00, 17:00) to capture diurnal heat exposure patterns. ENVI-met 5.7.1 was used to simulate microclimate parameters, including $T_a$, wind speed, and relative humidity, given its capacity for resolving mesoscale atmospheric exchanges in dense urban zones [32]. Its accuracy in estimating mean radiant temperature (MRT) has been validated in recent studies, which also highlighted ongoing challenges under hot-arid conditions [27]. $T_s$, MRT, and UTCI were calculated using Ladybug Tools v1.8 within Grasshopper, which allows high-resolution parametric radiation modeling and index derivation [22], [36]. The choice of tools aligns with hybrid workflows highlighted in systematic reviews of thermal comfort assessments under morphological constraints [35].

Each albedo scenario was modeled using fixed inputs and processed through a standardized simulation. Thermal performance was interpreted using UTCI's thermal stress bands, which have been regionally adapted in hot-arid urban studies [19]. Analytical comparisons focused on evaluating the performance of ENVI-met in reproducing key thermal comfort indicators (including Ta, Ts, MRT, and UTCI) through validation against field measurements [24], [33].

Simulated outputs were processed using consistent visual and numerical analytics across all scenarios. $T_a$ and MRT values were benchmarked against empirical measurements collected on-site and via globe thermometer-based MRT estimation. UTCI was derived using Ladybug's comfort calculator component, integrating the validated microclimate inputs [22], [34].

## 2.2. Location and Case Study Description

This study investigates a commercial pedestrian strip located within a gated residential compound in New Cairo, Egypt. As shown in Figure 2, the site typifies the urban morphology of newly developed districts across hot-arid regions, characterized by wide vehicular roadways, minimal vegetation, and a dominance of hardscape surfaces. These spatial configurations exacerbate surface heating and elevate radiant exposure, particularly during peak insolation hours, thereby diminishing outdoor thermal comfort [36].

The strip adopts a north–south orientation and is bounded by retail blocks of uniform height, arranged to maximize visual symmetry and commercial branding. However, the space lacks any vegetative or architectural shading elements, resulting in a sky view factor approaching unity. This full-sky exposure, combined with the absence of trees, shading canopies, or evaporative features, effectively isolates surface material reflectivity as the principal microclimatic modifier. Such design characteristics reflect a broader regional trend wherein visual uniformity is prioritized over environmental responsiveness in upscale developments across the MENA region [6], [21].

The paving palette comprises predominantly Triesta Grey Marble and dark basalt, materials favored for their aesthetic qualities but characterized by low albedo and high thermal mass. As shown in Figure 3, these materials are distributed throughout the pedestrian path, while asphalt is used as the pavement material for the adjacent vehicular lanes. To incorporate these material properties into the simulation framework, both materials had a similar albedo of 0.12; therefore, this value was unified as the base case albedo. This simplification was made to represent the pavement with a single albedo value, allowing for a consistent increase along the pedestrian path in the two subsequent measurement scenarios.

On-site photographic documentation as shown in Figure 3 reinforces the strip's thermally aggressive design. The images highlight the persistent absence of passive cooling features (such as vegetative buffers, colonnades, or water elements) and highlight the dominance of heat-absorptive surfaces throughout the pedestrian realm.

From a methodological standpoint, the strip satisfies key criteria for isolating the thermal effects of albedo variation: a consistent street canyon geometry, minimal topographical variation, and homogenous material application. These characteristics align with case-selection principles in hot-arid street-canyon assessments [35].

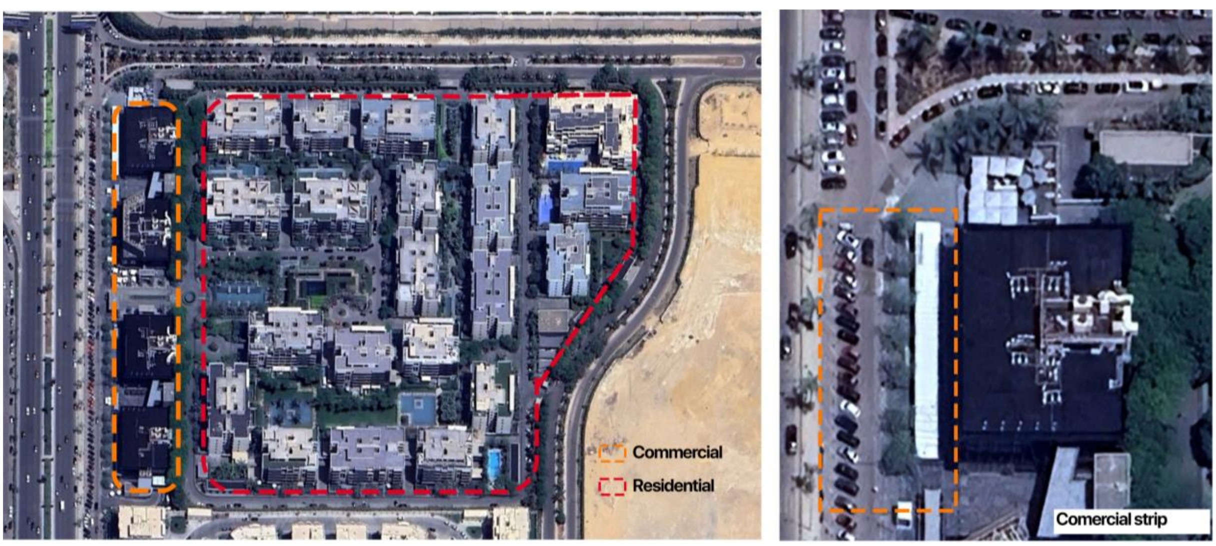


**Figure 2.** Google Earth image showing the layout of the commercial strip and the surrounding residential compound

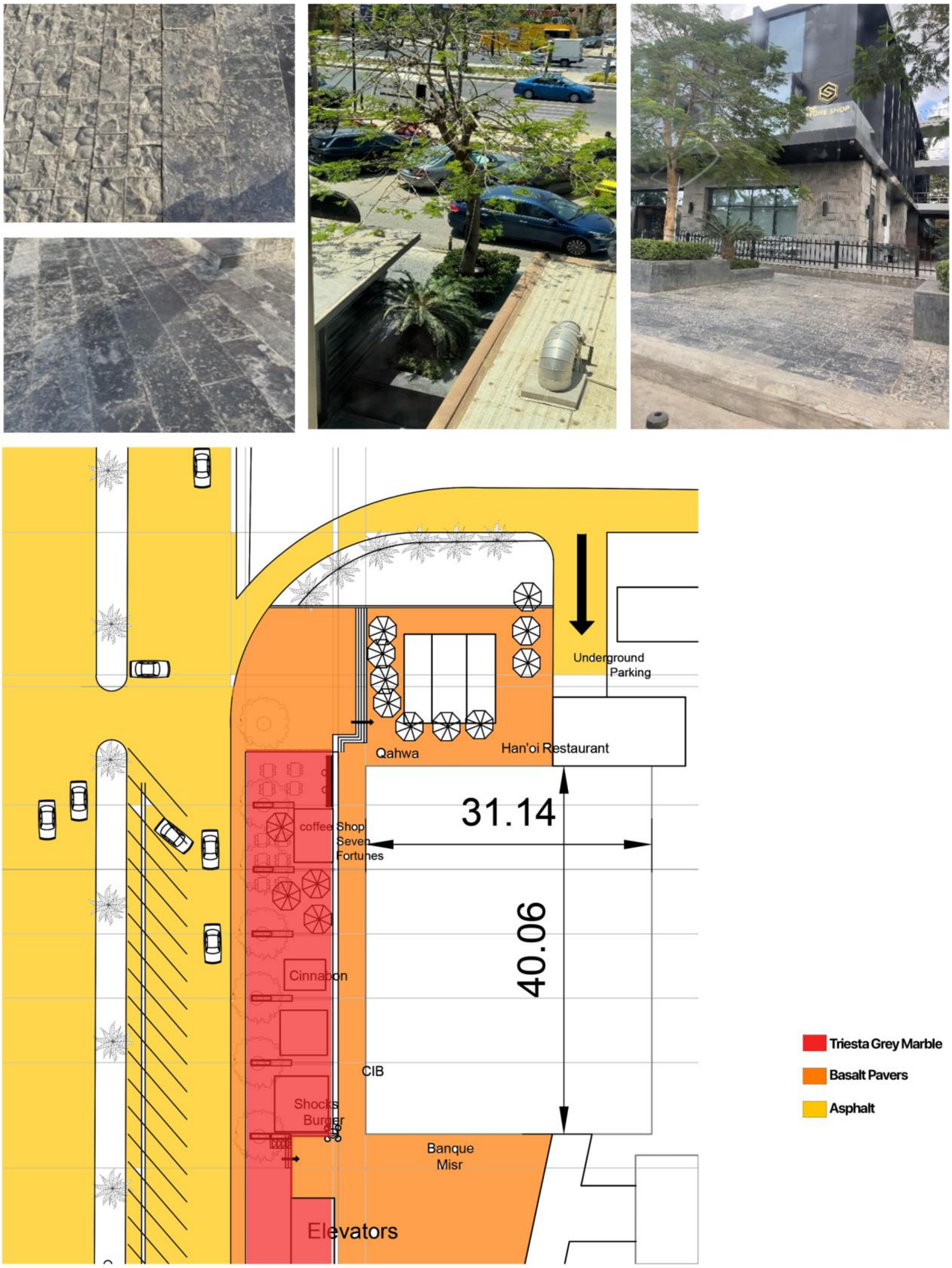


**Figure 3.** Main pedestrian path and on-site photographs showing the paving materials used in the case study area, including Triesta Grey Marble and dark basalt tiles

By focusing on a high-exposure, aesthetically driven strip typical of contemporary upscale districts in hot-arid cities, this study targets a development typology that routinely overlooks passive thermal regulation. The findings are thus applicable to similar urban morphologies seeking to balance commercial design with climatic resilience, including the integration of reflective and vegetation-based cooling strategies [5], [16], [20], [25]

### 2.3. Simulation Tools

To capture the thermal behavior of the urban environment with high spatial and temporal resolution, a hybrid simulation workflow was employed, integrating ENVI-met 5.7.1 with Rhinoceros 3D and its parametric environment Grasshopper, powered by Ladybug Tools v1.8. This dual-platform strategy allowed the study to leverage ENVI-met's microclimatic fidelity and Grasshopper's parametric flexibility to evaluate thermal comfort under varying surface albedo conditions. Such an integrated method aligns with validated urban thermal modeling frameworks adopted in recent hot-arid studies [23], [33], [35].

ENVI-met was selected for its ability to simulate three-dimensional microclimatic parameters (including Ta, wind speed (WS), and relative humidity (RH)) within a built environment context, and its outputs have been validated against field measurements in hot-arid conditions [27]. The simulation domain was constrained to 50 × 50 m due to software limitations, focusing on a representative sub-zone characterized by maximum solar exposure and minimal vegetative cover. The model resolution (2 m horizontal, 0.5 m vertical) was designed to capture detailed thermal patterns at pedestrian height (1.4 m), a critical threshold for outdoor comfort evaluation.

ENVI-met inputs included meteorological data (air temperature, RH, wind speed) from field measurements, boundary conditions fixed for summer peak, and surface material properties (albedo, emissivity). Outputs included pedestrian-level Ta, Ts, and WS at 1.4 m resolution. Grasshopper/Ladybug inputs included geometry, albedo values, and solar position. Outputs included MRT and UTCI. Assumptions included constant geometry and no vegetation to isolate albedo effects.

Simultaneously, the full-scale geometry of the commercial strip was reconstructed in Rhinoceros 3D, with the Grasshopper interface enabling precise control over building forms, surface materials, and solar exposure conditions. Ladybug Tools facilitated the simulation of key thermal indices:

- Mean Radiant Temperature (MRT) was modelled using the 'Outdoor Solar MRT' module, which incorporates solar position, surface reflectivity, and sky view factor to estimate longwave and shortwave radiation loads. This approach mirrors that of El Gendy et al. [6], who emphasized MRT as a dominant factor in thermal discomfort in unshaded urban settings, a finding consistently reinforced in systematic reviews [35]. This is especially relevant when high-albedo surfaces repel shortwave radiation back toward the pedestrian body, intensifying radiant exposure despite reductions in surface or Ta; a dynamic strongly influenced by surrounding urban morphology [37].
- Universal Thermal Climate Index (UTCI) was derived using Ladybug's comfort calculator, integrating ENVI-met-generated Ta, RH, and WS with Grasshopper-derived MRT. This method of hybrid computation has been validated for accuracy in climate-responsive design testing [33].
- $T_s$ was computed based on solar radiation analysis and material-specific thermal properties, with parameters such as emissivity and absorptance sourced from literature and calibrated field observations [6], [10].

The hybrid modeling setup is shown in Figure 4. The ENVI-met grid (left) depicts detailed spatial patterns of thermal loads in a constrained environment, while the Rhino-Grasshopper model (right) represents the broader urban morphology, enabling scalable simulations across variable albedo scenarios.

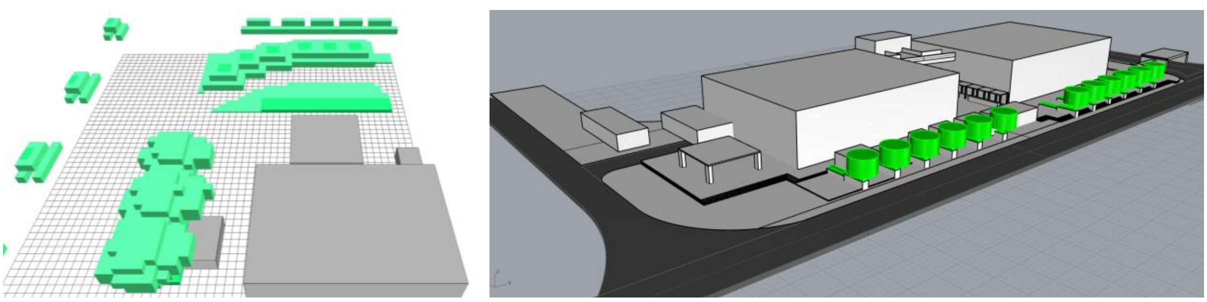

Model in Envi met Model in Rhino

**Figure 4.** Left is the ENVI-met simulation grid of the commercial strip displaying vegetative and built elements. Right: Rhino 3D reconstruction highlighting commercial zones and pedestrian walkways used in reflectivity scenarios

This simulation approach follows the workflow outlined and validated in El Gendy et al.'s 2025 study, which integrates ENVI-met with parametric modeling tools [6], [21]. By decoupling the environmental micro-scale simulation from broader parametric controls, this dual-software method allows for both empirical precision and scenario adaptability [13], [35], [38]. The use of ENVI-met as a climatic input layer and Grasshopper as a thermal comfort testing environment has been increasingly recognized as a robust framework for urban climate-sensitive research in arid contexts [6], [21], [22]. This aligns with Kamel's Egypt-focused workflow, which formalized the integration of parametric tools and microclimatic simulations for more adaptable, high-resolution outdoor comfort analysis [21].

### 2.4. Simulation Process

The simulation process was structured to ensure consistency, isolate variables, and validate thermal comfort metrics under peak summer conditions in New Cairo. It began with digital reconstruction of the full commercial strip in Rhinoceros 3D, based on field measurements, architectural documentation, and photographic references. Spatial elements, including buildings, paving extents, and surrounding open areas, were modeled to scale, ensuring accurate representation of the site's morphological and material properties.

To simulate microclimatic conditions, a representative $50 \times 50$ m subdomain was selected and imported into ENVI-met Spaces 3D. The subdomain was chosen for its high solar exposure, minimal shading, and absence of vegetative modifiers; ideal conditions for isolating the thermal effect of surface reflectivity. ENVI-met 5.7.1 was used to simulate $T_a$, wind speed (WS), and relative humidity (RH) at a 1.4 m pedestrian level across five critical time intervals (09:00–17:00), consistent with methods employed in regional heat stress analyses [23], [28].

Validated ENVI-met outputs were then exported and processed within the parametric model in Grasshopper, where three surface reflectivity scenarios (albedo values of 0.12, 0.20, and 0.30) were modeled across the strip. All other parameters, including geometry, meteorological inputs, and material configuration, were held constant to maintain experimental control. This approach parallels the methodological isolation techniques outlined in recent urban climate studies on reflective pavement strategies [15], [25].

Rather than relying on EPW-based weather inputs alone, the integration of ENVI-met's spatially resolved data enhanced the fidelity of Mean Radiant Temperature (MRT) and Universal Thermal Climate Index (UTCI) calculations, as validated under extreme heat conditions [33]. Simulations were conducted at three peak exposure hours (11:00, 13:00, and 15:00), corresponding to solar altitude maxima and heightened pedestrian activity. This timing aligns with validated calibration windows used in comparable hot-arid climate studies [39], and with GIS-based urban microclimate mapping practices that sample diurnal extremes to resolve exposure hotspots [40].

Post-processing outputs focused on quantifying thermal responses across the three scenarios. Metrics were extracted at consistent pedestrian nodes and visualized through time-series plots and comparative heatmaps. This ensured that any observed cooling in Ta was due to suppressed surface convection, while increases in MRT could be attributed to shortwave repulsion off high-albedo materials, a response modulated by surrounding urban morphology [37]. By maintaining constant environmental geometry and simulating identical conditions across all cases, the study ensured that differences in Ta, MRT, and UTCI were attributable solely to changes in surface albedo [4], [5], [6]. This logic of variable isolation mirrors the comparative framework proposed by El Gendy et al. in their assessment of albedo's thermal implications in suburban Cairo and is consistent with simulation-based frameworks used to evaluate morphology-driven comfort outcomes [6], [37].

Finally, thermal stress was classified using UTCI bands defined in international literature and validated for local applicability in dense urban environments [17], [34]. The results informed both the quantitative analysis and the interpretation of trade-offs between surface cooling and radiant heat exposure.

### 2.5. Validation of the Model

To ensure the accuracy and credibility of the simulation results, a validation was implemented. This involved simulation outputs from ENVI-met 5.7.1 and Ladybug Tools against field measurements collected on August 15, a peak summer day representative of extreme outdoor conditions in New Cairo. The process specifically targeted Mean Radiant Temperature (MRT) and $T_a$, the two primary indicators of pedestrian thermal stress [17].

As shown in Figure 5, field data were collected using ISO 7726:1998 compliant instruments, mounted at approximately 1.4 m above ground level to represent pedestrian exposure. Instruments included:

- **Testo 435-2 Indoor Air Quality Meter** (temperature range −20 °C to +70 °C, accuracy ±0.5 °C, RH range 0–100%, accuracy ±2%).
- **Extech EasyView IAQ Meter** (temperature range −30 °C to +60 °C, accuracy ±0.6 °C).
- **Hot-wire thermo-anemometer** (range 0–20 m/s, accuracy ±0.03 m/s).
- **Black globe probe Testo 0602 0743** (diameter 150 mm, emissivity 0.95, accuracy ±0.3 °C).

$T_a$ and relative humidity (RH) were measured using both the Testo 435-2 Indoor Air Quality Meter (Figure 5B) and the Extech EasyView IAQ Meter (Figure 5C) to ensure cross-validation of environmental readings.


A: black globe probe (Testo 0602 0743) B: Testo 435-2 Indoor Air Quality Meter C: Extech EasyView IAQ Meter D: Hot-wire thermo-anemometer

**Figure 5.** The instruments used in data collection for validation

Wind speed (WS) was recorded using a hot-wire thermo-anemometer (Figure 5D), selected for its sensitivity in capturing low-speed airflow critical to thermal comfort modeling. Mean Radiant Temperature (MRT) was not measured directly; it was manually calculated using the ISO 7726–based formula, incorporating globe temperature, $T_a$, and wind speed. Globe temperature was obtained via a black globe probe (Testo 0602 0743) connected to the Testo 435-2 (Figure 5A).

### 2.6. MRT Validation Using Ladybug Tools

MRT values were simulated using Ladybug Tools within Grasshopper, based on solar radiation inputs and customized environmental boundary conditions, consistent with GIS-based evaluation methods applied in recent comfort studies [22]. Simulation outputs were validated against field measurements derived from black globe temperature readings using the standard ISO 7726 formula, incorporating wind speed, globe diameter, and emissivity. Recent studies have further confirmed the advances and challenges of MRT validation in ENVI-met simulations [41].

R-squared ($R^2$) is a statistical indicator used to assess the correlation strength between simulation results and actual measurements. Mean Radiant Temperature (MRT) simulation results from Grasshopper were validated against field measurements, yielding an $R^2$ value of 0.924. This indicates a strong correlation with reasonable accuracy, reflecting high alignment in early hours and a slight overestimation during late afternoon as shown in Table 1.

The results exhibited a strong linear correlation as shown in (Figure 6) with a coefficient of determination ($R^2$) exceeding 0.924, confirming the accuracy of Ladybug's simulation capabilities [42], [43]. These findings are consistent with recent ENVI-met case studies on street canyon geometry, which also demonstrated strong predictive performance under extreme hot-weather conditions [42]. This validation approach aligns with earlier studies that employed hybrid simulation techniques in hot-arid regions, where Ladybug was integrated with site data to enhance accuracy under high-radiation conditions [36].

### 2.7. $T_a$ Validation Using ENVI-met

$T_a$ values simulated by ENVI-met at 1.4 m above ground level were extracted and compared against field measurements recorded at matching intervals on August 15, a peak summer day in New Cairo. The comparison yielded a strong correlation, with a coefficient of determination ($R^2$) of 0.984, demonstrating peak alignment during midday hours (Figure 7) [6], [43], [44].

These results fall within the recognized accuracy range of ENVI-met, particularly under hot-arid conditions where minor underestimation biases have been previously reported [41]. The 1.4 m simulation height aligns with best practices for evaluating thermal comfort at the pedestrian level, as established in outdoor urban microclimate studies [44]. The model's performance is also consistent with prior validation efforts across MENA contexts, where limited vegetation and high surface reflectivity often amplify thermal load and minimize convective modulation. Similar outcomes have been documented in arid canyon-type environments, validating ENVI-met's applicability in morphology-driven comfort assessments [24], [27], [31], [44].

Minor discrepancies between ENVI-met and Grasshopper outputs were observed, with Grasshopper slightly overestimating MRT during late afternoon. These differences were addressed through calibration with field data and sensitivity checks. The high correlation coefficients ($R^2 = 0.924$ for MRT, $R^2 = 0.984$ for Ta) confirm model validity.

This study contributes by addressing the common reliance on dark luxury materials such as basalt in Egypt's outdoor spaces, which intensifies heat stress. The contribution lies in improving material selection to enhance outdoor thermal comfort through a hybrid modelling integration of ENVI-met and Ladybug Tools. ENVI-met was applied for microclimatic data at the small-scale (restricted to 50 × 50 m), and these outputs were subsequently used as inputs for Ladybug, which is capable of simulating larger urban domains such as neighbourhoods and full street corridors. This workflow leverages the strengths of both models, providing a more comprehensive framework for assessing the impacts of reflective pavements on thermal comfort in hot-arid environments.

**Table 1.** Comparison of field-measured and Grasshopper-simulated MRT values

| **Time** | **Mean Radiant Temperature °C Measured** | **Mean Radiant Temperature °C Simulated** |
|---|---|---|
| 9:00 | 52.01 | 50.2 |
| 11:00 | 62.9 | 64.5 |
| 13:00 | 66.8 | 70.2 |
| 15:00 | 69.8 | 71.6 |
| 17:00 | 58 | 63.1 |

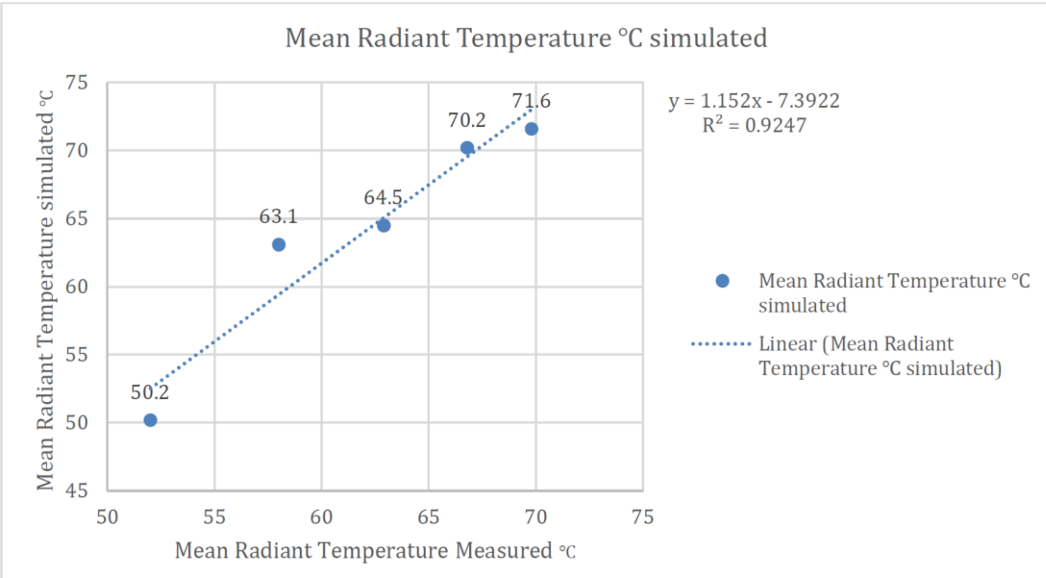


**Figure 6.** The R-squared ($R^2$) Value between Measured and Simulated MRT

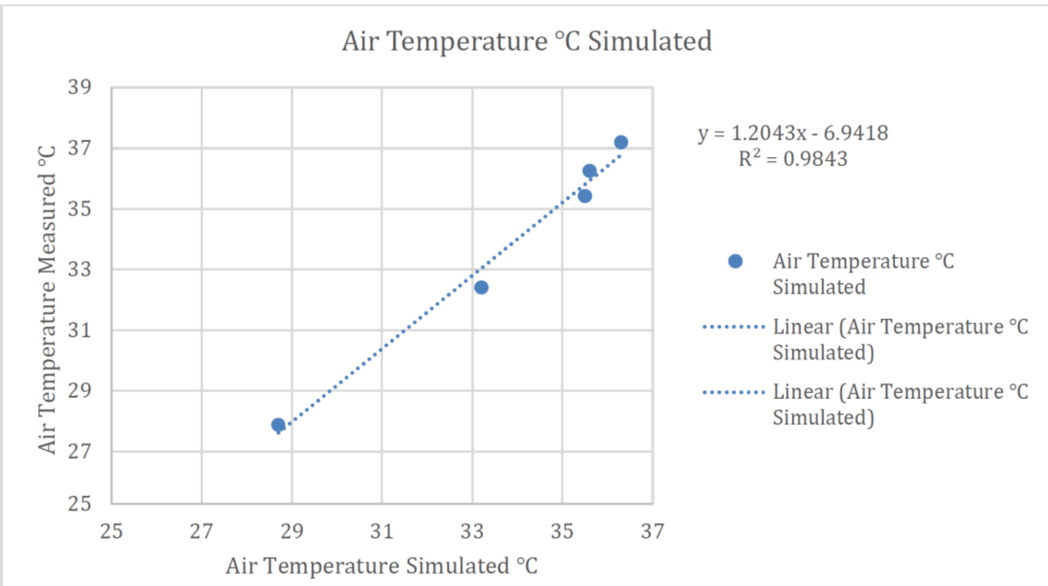


**Figure 7.** The R-squared ($R^2$) Value between Measured and Simulated $T_a$

### 2.8. Scenario Control and Albedo Consistency

To isolate the thermal effects of surface reflectivity, three albedo scenarios were modeled: 0.12, 0.20, and 0.30. All other boundary conditions (including urban geometry, sky view factor, vegetation, and material thickness) were held constant across simulations [6]. Only surface reflectivity (albedo) and its inverse, absorptance, were modified across the cases.

This approach aligns with validated experimental protocols used in reflective material studies, where spatial and climatic variables are strictly controlled to ensure accurate attribution of thermal responses to surface properties [4], [25], [34]. The selected albedo values reflect typical urban surfaces found in Cairo, ranging from dark asphalt (0.12) to polished stone (0.20), and light-colored engineered pavements (0.30) [6].

Comparable albedo ranges have been used in thermal comfort studies across hot-arid and semi-arid cities such as Tehran and Gulf cities, allowing for cross-contextual benchmarking and comparative analysis of pedestrian comfort outcomes [12], [13], [23], [26].

## 3. Results

### 3.1. Air Temperature

Air temperature ($T_a$) serves as a key indicator in assessing outdoor thermal conditions, especially in hot-arid climates where reduced convective cooling intensifies pedestrian heat exposure. While not the sole determinant of thermal comfort, Ta influences physiological stress and remains a central input in thermal indices such as the Universal Thermal Climate Index (UTCI).

Hourly $T_a$ was simulated at pedestrian height (1.4 m) across three surface albedo scenarios: 0.12 (dark basalt), 0.20 (medium tone paving), and 0.30 (light-colored reflective stone), as shown in Figure 8. All other environmental variables were held constant to isolate the influence of surface reflectivity on microclimatic air behavior.

At 9:00, Ta was 28 °C under the base case albedo 0.12, compared to 27.5 °C under 0.20 and 27.0 °C under 0.30; a 1.0 °C reduction between the extreme cases.

At 11:00, the values were 33 °C, 32.5 °C, and 32.0 °C, respectively, again showing a 1.0 °C cooling from the base.

At 13:00, temperatures were 36 °C (0.12), 35.5 °C (0.20), and 35.0 °C (0.30), confirming a 1.0 °C drop between each increment.

The peak difference occurs at 15:00, where 0.30 achieved a 1.5 °C reduction versus the base case, with readings of 38 °C (0.12), 37.5 °C (0.20), and 36.5 °C (0.30).

By 17:00, $T_a$ was 37 °C, 36.5 °C, and 35.5 °C across the three surfaces, maintaining a 1.5 °C decrease between 0.12 and 0.30.

This consistent decline reflects the reduced convective heating above higher-albedo surfaces, which reflect more incoming shortwave radiation and absorb less heat. The observed reductions closely align with Aboelata's ENVI-met cool-paving results in Egyptian arid districts [45], as well as Faragallah and Ragheb's ENVI-met simulations in Egypt [19], where reflective pavements yielded Ta drops of around 2 ℃.

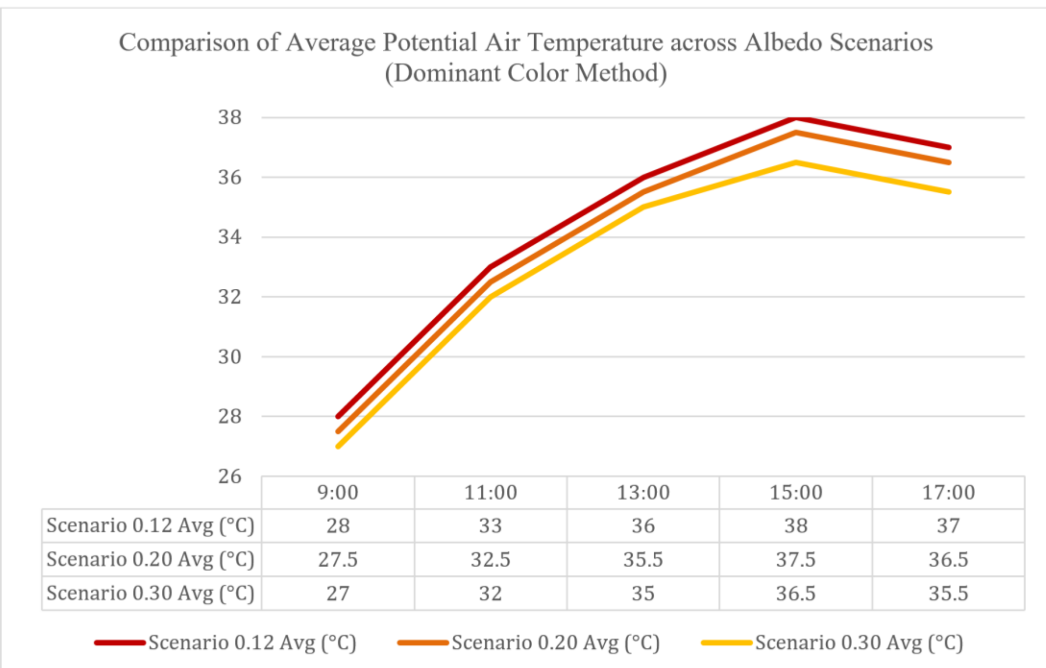


| | 9:00 | 11:00 | 13:00 | 15:00 | 17:00 |
|---|---|---|---|---|---|
| Scenario 0.12 Avg (°C) | 28 | 33 | 36 | 38 | 37 |
| Scenario 0.20 Avg (°C) | 27.5 | 32.5 | 35.5 | 37.5 | 36.5 |
| Scenario 0.30 Avg (°C) | 27 | 32 | 35 | 36.5 | 35.5 |

**Figure 8.** Hourly air temperature trends across different albedo scenarios (0.12, 0.20, 0.30)

However, despite this positive trend, the reductions remain moderate in magnitude, rarely exceeding 1.5 °C. These findings confirm that while high-albedo surfaces reduce convective heat buildup, their cooling effect on $T_a$ is constrained by ambient mixing, urban geometry, and the absence of evaporative cooling. Consequently, as explored in subsequent sections, albedo interventions must be coupled with vertical shading to offset the parallel rise in radiant exposure; a factor not captured by Ta alone.

### 3.2. Surface Temperature

$T_s$ is a direct thermodynamic response to solar radiation and plays a critical role in shaping local microclimatic conditions. In hot-arid environments such as New Cairo, midday solar intensity causes significant heat buildup on exposed surfaces, which directly affects pedestrian thermal comfort through both radiative and convective heat transfer.

Figure 9 shows diurnal $T_s$ patterns for three albedo scenarios (88%, 80%, and 70% solar absorptance) corresponding to albedo values of approximately 0.12, 0.20, and 0.30, respectively. The data reveal a consistent inverse relationship between surface reflectivity and Ts throughout the day.

At 9:00, $T_s$ in the base case (88% absorption) reached 31.5 °C, while both medium- and high-reflectivity surfaces recorded 28.5 °C, indicating a 3 °C reduction due to increased solar reflection. By 11:00, Ts rose sharply to 46 °C for the low-albedo surface, compared to 42.5 °C (80%) and 40.1 °C (70%), further demonstrating the cooling effect of high-albedo materials.

The most significant thermal divergence occurred at 13:00, when the 88% absorption surface peaked at 58.2 °C, while the high-albedo 70% surface measured 51.25 °C; yielding a 7 ℃ reduction. These findings are consistent with López-Cabeza et al. [46], who reported substantial Ts reductions when reflective pavements were applied in Mediterranean urban contexts. Similarly, Aboelata [45] reported that reflective pavements in arid Egyptian districts produced Ts reductions of up to 6 ℃ under peak summer conditions. Complementary analyses confirm that pavement radiative and thermal properties critically influence these outcomes, shaping both immediate and long-term Ts performance [30].

At 15:00, the cooling effect persisted, with Ts values measuring 54 °C, 50.5 °C, and 48.46 °C across the three scenarios, respectively. By 17:00, $T_s$ began to converge due to declining solar incidence, though the high-albedo surface maintained a slight thermal advantage, staying nearly 1 °C cooler than the base case.

These trends, depicted in Figure 9, confirm the capacity of reflective surfaces to reduce thermal accumulation during peak solar load periods. Recent field validation studies in high-density urban settings similarly demonstrated the cooling benefits of reflective materials, affirming the broader applicability of material-based passive cooling strategies [34].

In summary, the $T_s$ analysis confirms that increasing albedo through material selection is an effective passive cooling strategy. However, Ts reduction alone does not guarantee improved pedestrian thermal comfort, which also depends on Mean Radiant Temperature and UTCI; metrics will be addressed in the following sections [47].

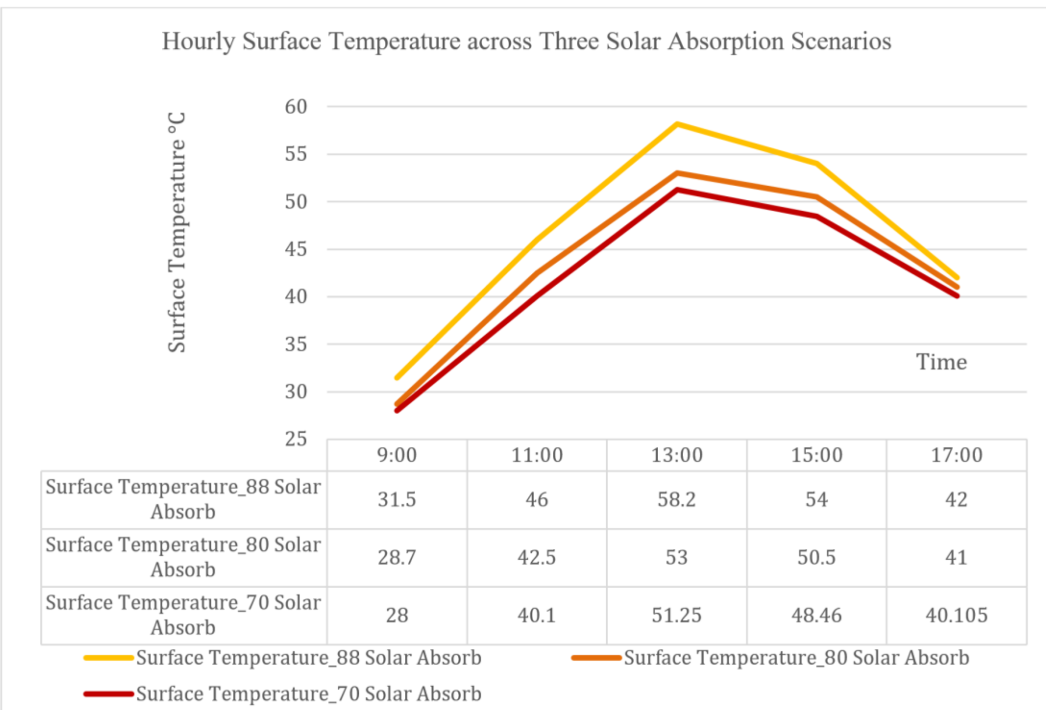


| | 9:00 | 11:00 | 13:00 | 15:00 | 17:00 |
|---|---|---|---|---|---|
| Surface Temperature_88 Solar Absorb | 31.5 | 46 | 58.2 | 54 | 42 |
| Surface Temperature_80 Solar Absorb | 28.7 | 42.5 | 53 | 50.5 | 41 |
| Surface Temperature_70 Solar Absorb | 28 | 40.1 | 51.25 | 48.46 | 40.105 |

**Figure 9.** Hourly surface temperature across three surface types with varying solar absorption rates (88%, 80%, 70%)

### 3.3. Mean Radiant Temperature (MRT)

Mean Radiant Temperature (MRT) quantifies the cumulative effect of all radiant fluxes acting on the human body, combining both direct solar shortwave and re-radiated longwave radiation from surrounding surfaces. It plays a critical role in thermal perception, particularly in hot-arid urban contexts where solar radiation significantly outweighs convective heat transfer [29].

MRT values were simulated at five key time points (9:00, 11:00, 13:00, 15:00, and 17:00) under three albedo scenarios: 0.12 (dark basalt), 0.20 (medium reflectivity), and 0.30 (light reflective stone). The results shown in Figure 10, show a clear trend of increasing MRT with higher albedo throughout the day, particularly during midday hours when solar incidence peaks.

At 9:00, MRT under albedo 0.12 was 51 °C, rising to 53.45 °C and 55.95 °C under albedos 0.20 and 0.30, respectively. This early increase reflects the shortwave radiation repulsion effect characteristic of reflective materials, where incident solar radiation is redirected toward the pedestrian body, intensifying thermal exposure even in morning hours [6], [16], with exposure levels further shaped by surrounding urban morphology [37].

MRT continued to rise sharply by 11:00, reaching 63 °C (0.12), 65 °C (0.20), and peaking at 68.3 °C under the highest albedo (0.30), marking an early onset of radiant stress.

The most critical differences were recorded during peak solar hours. At 13:00 and 15:00, MRT reached 70 °C and 71 °C, respectively, under the base case 0.12 albedo. In contrast, MRT under the 0.30 albedo condition peaked at 72 °C for both time points, with the 0.20 surface trailing slightly behind.

By 17:00, MRT levels dropped to 63 ℃ (0.12), 66 ℃ (0.20), and 68.3 ℃ (0.30), indicating that even during declining solar angles, highly reflective surfaces sustain elevated MRT levels through continued shortwave repulsion [16], with GIS-based assessments confirming that such elevated exposures remain significant in urban resting spaces [40].

Physiologically, MRT > 60 ℃ coupled with Ta > 35 ℃ typically produces UTCI values in the very strong to extreme heat-stress range; this interpretation follows the operational UTCI framework [47]. The persistence of MRT above 70 ℃ under high-albedo surfaces highlights the need for shading structures and vegetated covers to reduce radiant load and improve comfort [38], [42], and the efficacy of albedo measures depends on morphology, reinforcing the need for complementary shading/vegetation [5]. Recent ENVI-met canyon studies under extreme heat conditions have shown similar MRT exceedances and emphasized the role of shading integration [42].

In conclusion, while high-albedo surfaces contribute to cooling through reduced heat storage and convection, they simultaneously intensify radiant heat through shortwave reflection. This reinforces that trade-off identified in hybrid simulation studies and highlights the importance of integrating vertical shading with surface-level interventions [5], [42]. Case studies of arid street canyons similarly confirm this trade-off between albedo-driven cooling and MRT intensification [42].

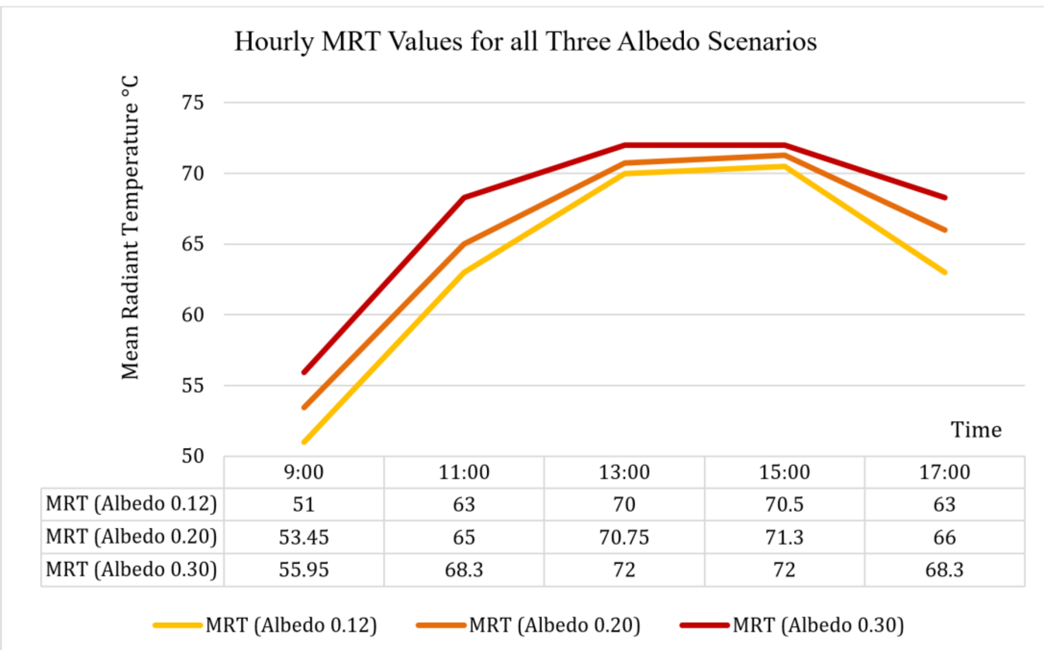


**Figure 10.** Displays the MRT profile throughout the day across all three albedo scenarios

### 3.4. Universal Thermal Climate Index (UTCI)

The Universal Thermal Climate Index (UTCI) is a composite indicator that evaluates outdoor thermal stress by integrating $T_a$, mean radiant temperature (MRT), wind speed (WS), and relative humidity (RH). It offers a physiologically relevant measure of human thermal perception in outdoor settings, particularly suited for hot-arid climates like New Cairo where high solar exposure and low evapotranspiration prevail.

Figure 11 presents UTCI simulations conducted at five key intervals (9:00, 11:00, 13:00, 15:00, and 17:00) across three surface albedo conditions: 0.12, 0.20, and 0.30. These values reflect the dynamic interplay between lower convective heating from high-albedo surfaces and increased shortwave reflection, which amplifies MRT and consequently UTCI [48], [49].

At 9:00, UTCI values were relatively moderate: 34.5 °C (0.12), 35.0 °C (0.20), and 35.2 °C (0.30). Despite low solar altitude, the 0.30 scenario showed a 0.7 °C increase over the base case, attributed to early-onset shortwave repulsion that elevated MRT [48], [49].

By 11:00, UTCI rose sharply to 40.3 ℃, 41.4 ℃, and 42.5 °C, all within the 'very strong' heat-stress category under standard UTCI thresholds [17] (see operational use [47]). The 2.2 ℃ differential between 0.12 and 0.30 highlights the impact of elevated MRT from high-albedo surfaces during mid-morning exposure [49].

At 13:00, UTCI values peaked at 44.7 °C for both the 0.12 and 0.20 cases, and 45.4 °C for 0.30. Although the rise appears smaller here, the cumulative heat load on pedestrians was significantly higher under high albedo surfaces due to sustained shortwave reflection [22], [48].

The most critical readings occurred at 15:00, with UTCI values reaching 46.0 °C (0.12), 46.2 °C (0.20), and 46.9 °C (0.30), According to the UTCI operational framework, these values fall within UTCI's operational categories (46.0 ℃ as very strong, 46.2-46.9 ℃ as extreme) per the UTCI framework used in European forecasting systems [47]. The 0.9 °C increase from the base case further shows the paradox of higher albedo: although air and $T_s$ decrease, the repulsion of shortwave radiation elevates MRT and UTCI [22], [49].

By 17:00, UTCI values began to taper, falling to 41.75 °C (0.12), 42.0 °C (0.20), and 42.5 °C (0.30). Nonetheless, the 0.75 °C gap between extreme cases indicates that radiant load from high-albedo surfaces persists even during declining solar angles [34].

These trends, shown in Figure 11, confirm that increased surface reflectivity intensifies perceived thermal stress despite moderate reductions in air and $T_s$. Similar outcomes were observed in simulation studies by Chen et al. [49] and Ibrahim et al. [22] (Ladybug verification) and are consistent with the broader evidence synthesized by Shooshtarian et al. [48].

In conclusion, the UTCI analysis reinforces that albedo enhancement alone cannot ensure thermal comfort [9]. The simultaneous rise in MRT under high-albedo conditions leads to greater pedestrian heat stress, especially during midday. To counter this, albedo strategies must be supplemented with vertical shading or vegetative coverage, echoing best-practice recommendations for climate-responsive urban design [5].

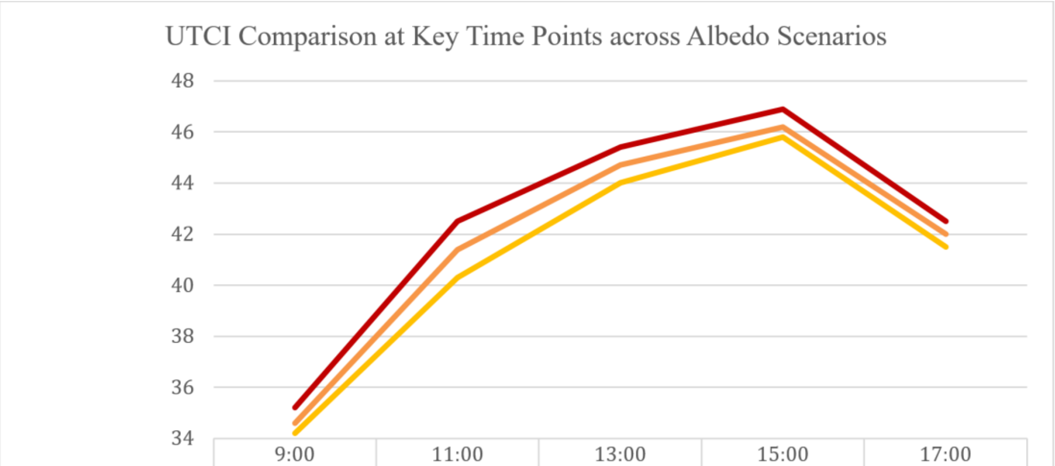


| | 9:00 | 11:00 | 13:00 | 15:00 | 17:00 |
|---|---|---|---|---|---|
| UTCI _0.12 albedo | 34.2 | 40.3 | 44 | 45.8 | 41.5 |
| UTCI _ 0.2 albedo | 34.6 | 41.4 | 44.7 | 46.2 | 42 |
| UTCI_ 0.3 albedo | 35.2 | 42.5 | 45.4 | 46.9 | 42.5 |

**Figure 11.** Hourly variations in Universal Thermal Climate Index (UTCI) across three surface albedo scenarios (0.12, 0.20, 0.30)

### 3.5. Post-Albedo Shading Intervention

To address the elevated thermal stress associated with high-albedo surfaces (primarily due to increased Mean Radiant Temperature (MRT) and Universal Thermal Climate Index (UTCI)), a modular shading intervention was developed and simulated. This intervention aimed to mitigate radiant heat exposure in unshaded pedestrian zones without altering the ground materials or urban form.

#### 3.5.1. Shading Design Description

The applied shading consists of clustered circular canopy modules installed above concrete seating zones along the pedestrian strip. Each cluster includes three vertically staggered canopy elements, ranging in height from 2.65 m to 2.87 m, and spaced at intervals of approximately 7.35m (Figure 12). The canopies are fabricated from white-coated wooden structures (combining high albedo and low thermal conductivity) to reflect shortwave radiation while minimizing heat conduction and re-radiation. Such material selections align with recommendations for passive cooling in high-exposure contexts.

Solar path analysis guided the spatial configuration of the canopies, prioritizing shade during peak solar exposure between 11:00 and 15:00 to maximize thermal performance.

#### 3.5.2. Thermal Impact

Simulation results demonstrated substantial UTCI reductions following the shading intervention. Under the 0.20 albedo scenario, UTCI at 11:00 declined from 41.4 °C to 35.3 °C: a 6.1 °C improvement. At 13:00 and 15:00, UTCI decreased from 44.7 °C to 39.05 °C, and from 46.2 °C to 40.95 °C, respectively (Figure 13). These reductions correspond with prior studies reporting UTCI drops of 4-6 °C in shaded environments during peak periods [45].

To review performance across surface reflectance conditions, the 0.30 albedo case was also analyzed. Similar UTCI reductions were observed: from 42.5 °C to 35.3 °C at 11:00, with midday and afternoon values reduced by over 5 °C (Table 2). This convergence across albedo conditions after shading suggests that vertical shading mitigates the microclimatic disparities induced by surface reflectivity [11], [42], [50]. In a hot-arid case study of Tehran, increasing urban vegetation cover by 10% reduced PET by approximately 9.36 ℃, while changes to building orientation produced the largest air-temperature decrease (≈ 1.69 °C) [50].

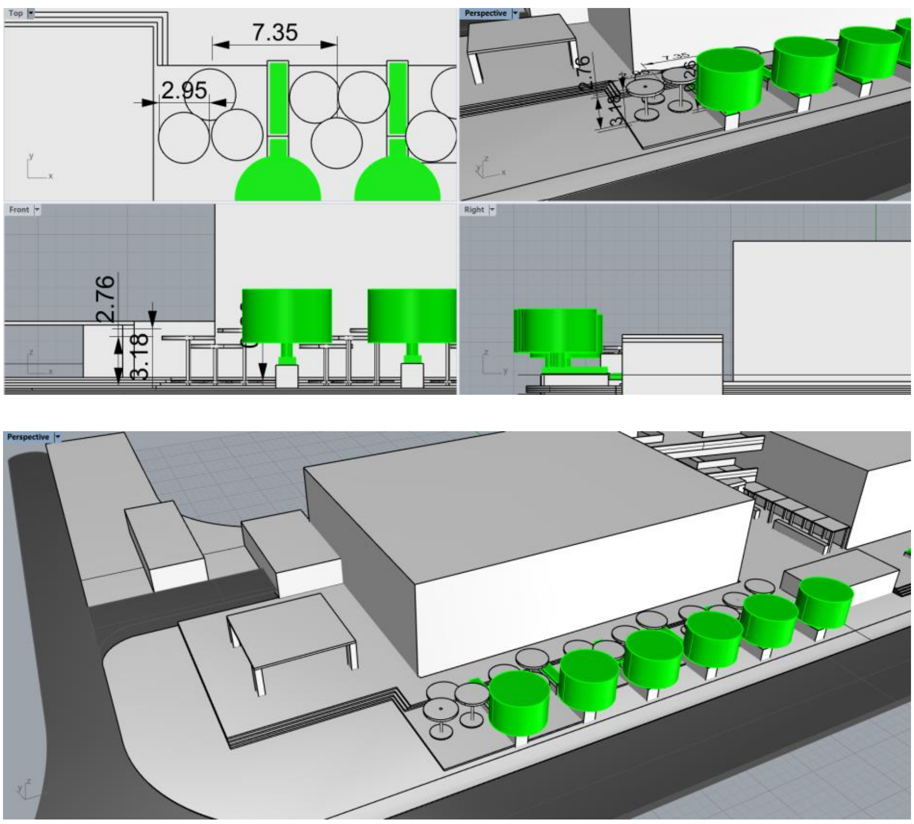


**Figure 12.** 3D Model of circular shading intervention in Rhino, Top Left: shows the Top view of the circular shading elements and their distribution, Top right: shows the 3D perspective and its connection to existing greenery, Bottom left: shows the front view showing the different height variation, Bottom Right: shows the right elevation where the shading is hidden behind the trees

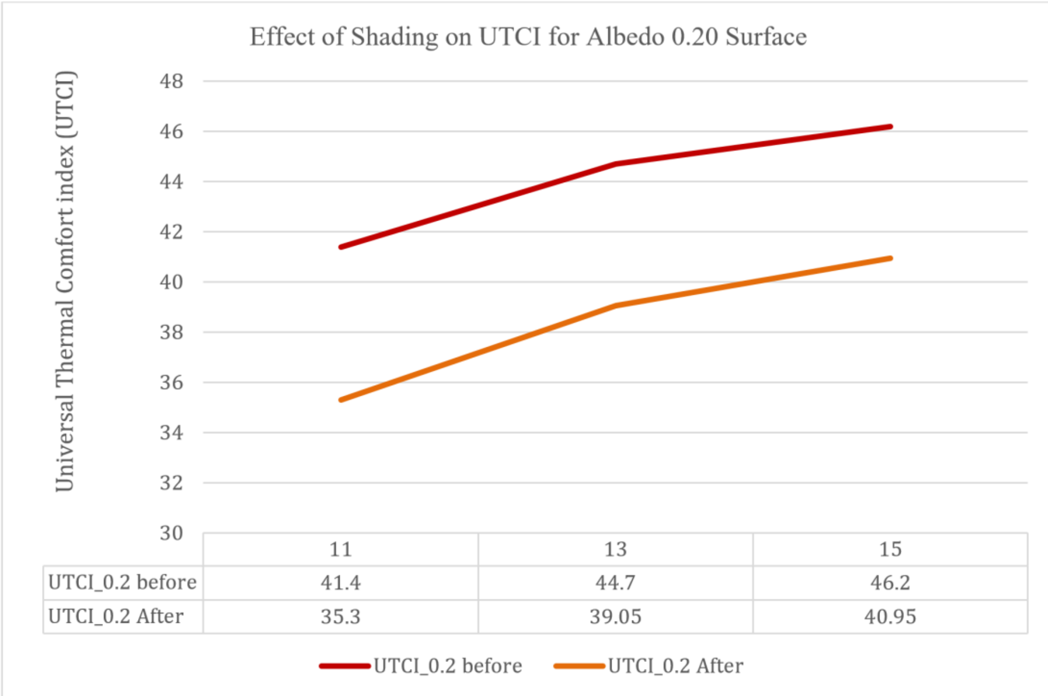


**Figure 13.** UTCI values before and after implementing shading structures for the Albedo 0.20 scenario

**Table 2.** UTCI values for the 0.30 albedo scenario

| Time | UTCI _0.3 before | UTCI _0.3 After |
|---|---|---|
| 11 | 42.5 | 35.3 |
| 13 | 45.4 | 39.05 |
| 15 | 46.9 | 40.95 |

The cooling effect is attributed to both geometric and material strategies. Canopy structures, for instance, can reflect incoming shortwave radiation while their low thermal mass limits longwave heat re-emission onto pedestrians, further reducing MRT and improving thermal perception; an effect consistently highlighted in parametric courtyard optimization studies [38].

These findings reinforce the assertion that while high-albedo materials influence surface and radiant heat dynamics, shading remains the dominant factor in regulating pedestrian-level comfort [51]. Post-intervention convergence in UTCI values across albedo cases confirms that vertical shading can neutralize reflectivity-induced thermal gradients. This aligns with urban design strategies emphasizing the synergy between reflective surfaces, shading devices, and vegetation for thermally adaptive public spaces [25], [50], [51]. Evidence syntheses and field guidance [4], alongside Mediterranean case studies [46], indicate that reflective pavements, while initially effective, may exhibit efficiency losses with exposure and use, underscoring the need for durability testing in both Mediterranean and arid climates.

This study's findings confirm that vertical shading plays a more decisive role in regulating outdoor thermal comfort than surface reflectivity alone. The implementation of modular canopy systems mitigated the rise in MRT and UTCI across all albedo scenarios, effectively harmonizing microclimatic conditions. These results are consistent with prior research emphasizing the critical synergy between reflective materials, shading devices, and vegetative elements in designing thermally adaptive public spaces [25], [50], [51].

# 4. Discussion

## 4.1. Thermal Effects of Surface Albedo on Air & Surface Temperatures

The simulation results confirm that increasing surface albedo effectively lowers both $T_s$ and near-ground $T_a$ during peak solar periods in hot-arid urban contexts like New Cairo [6]. At 15:00, $T_a$ decreased from 38 °C under the base case low-albedo surface (0.12) to 36.5 °C under the high-albedo condition (0.30), marking a 1.5 °C reduction. This pattern was consistent throughout the day, with incremental reductions observed at each time step, affirming the role of albedo in mitigating convective heating near pedestrian level [6]. This trade-off reflects the inherent radiative dynamics of reflective pavements, as highlighted in pavement thermal property studies [30].

$T_s$ exhibited even greater sensitivity to albedo variation. At 13:00, Ts reached 58.2 °C under 0.12, compared to 51.25 °C under 0.30, representing a 7.0 °C decrease. This is consistent with Mediterranean case studies, where Croce et al. [52] observed that reflective pavements reduced Ts by up to 14 ℃, reinforcing the cross-regional applicability of these findings, and with Aboelata [45], whose simulations in Egyptian arid districts reported surface temperature differences of approximately 6 ℃ between conventional and high-albedo pavements.

$T_a$ reductions remained modest in comparison, not exceeding 1.5-2 °C. This aligns with Aboelata's ENVI-met simulations in arid Egyptian districts (≈1-2 ℃ Ta decrease) [45], El Gendy et al.'s results (Ta 1-2 ℃; Ts 3-6 ℃) [6], and Faragallah and Ragheb's measurements (≈2 °C Ta decrease) [19] under similar conditions. The relatively small $T_a$ response highlights that reflective pavement, although effective in lowering Ts, cannot by itself ensure substantial improvements in pedestrian-level comfort.

The slight overestimation of MRT by Grasshopper during late afternoon hours is likely due to differences in how the two models handle radiative exchange: ENVI-met resolves short- and longwave radiation on a 3D grid with MRT performance validated in hot-arid and subtropical cases [27], [44], whereas the Grasshopper workflow relies on parametric solar-exposure models [33], [34] that can overestimate shortwave under clear, high-sun conditions. Similar tendencies were also noted in El Gendy et al. [6], who reported higher simulated MRT values from parametric workflows compared to field validation in Cairo. Despite this variation, both models showed strong alignment with field measurements, confirming the overall robustness of the dual-platform workflow.

In summary, enhancing surface albedo substantially reduces thermal storage and daytime Ts, offering localized cooling benefits. However, its effect on Ta is moderate and insufficient in isolation. These findings are consistent with ENVI-met validation studies, which found that reflective pavements provided short-term microclimatic relief [45] but required morphological or vegetative support to achieve sustained pedestrian comfort improvements [6], [33].

### 4.2. Impact on (MRT) and (UTCI)

While surface albedo enhancement effectively reduced $T_a$ and $T_s$, simulation results revealed a concurrent and significant increase in Mean Radiant Temperature (MRT) with higher reflectivity. At 9:00, MRT rose from 51.0 °C under the base albedo (0.12) to 55.95 °C under albedo 0.30; a 4.95 °C increase. By 15:00, MRT peaked at 72.0 °C for the highest albedo case, slightly exceeding the 71.0 °C recorded under the base case. This confirms that while high-albedo surfaces reduce ground-level heat storage, they simultaneously intensify shortwave reflection and increase radiant exposure for pedestrians [6], [16], [48].

These findings are consistent with the synthesis by Shooshtarian et al. [48]. Field analyses in Cairo indicate that MRT elevation is more pronounced in open urban zones where surface reflectivity redirects solar radiation [15]. Notably, MRT levels in this study frequently exceeded 60 ℃ between 11:00 and 15:00 across all scenarios, confirming exposure to very strong to extreme heat stress per standard UTCI categories [17]; this interpretation follows the operational UTCI framework [47].

UTCI outputs followed the same pattern, with heat stress intensifying under increased reflectivity. At 15:00, UTCI rose from 45.8 °C under albedo 0.12 to 46.9 °C under albedo 0.30, a shift from "strong" to "very strong" heat stress levels. At 11:00 and 13:00, UTCI values similarly increased with albedo, peaking at 42.5 °C and 45.4 °C, respectively, under albedo 0.30. These outcomes align with Liu et al. [5], who showed that UTCI is strongly influenced by radiant load and are consistent with operational UTCI assessments where shortwave reflection drives elevated stress [47].

The decoupling of MRT from $T_a$ in this study highlights a critical trade-off: while albedo modifications can yield modest air cooling (1-1.5 °C), the simultaneous rise in MRT often offsets these benefits at the pedestrian level. This aligns with field evidence from Cairo [15], where reflective pavements increased solar exposure and counteracted $T_a$ cooling.

Consequently, these results support a key conclusion echoed in prior studies [6], [5], [48], that albedo optimization, in isolation, is insufficient for achieving thermal comfort in exposed outdoor settings. Complementary strategies such as shading and vegetation are essential to mitigate radiant heat loads and ensure consistent comfort improvements. Without such integration, reflective pavements risk exacerbating pedestrian heat stress during peak solar hours [4].

Overall, the discussion confirms that while albedo-based strategies provide measurable cooling benefits, their trade-offs in terms of increased radiant load cannot be overlooked. The findings emphasize the need for multi-variable design solutions where albedo is embedded within broader passive cooling frameworks that include shading, vegetation, and morphological adaptation. This reinforces the consensus in recent studies [4], [5], [48] that reflective pavements should be evaluated not as stand-alone interventions but as part of integrated urban heat mitigation strategies.

## 5. Conclusions

This study demonstrates that surface albedo is an important but insufficient factor for improving pedestrian thermal comfort in hot-arid urban settings. While reflective pavements reduced surface and air temperatures by up to 7 ℃ and 1.5 ℃, respectively, these benefits were counteracted by elevated Mean Radiant Temperature and UTCI values under unshaded conditions. The canopy shading intervention proved far more decisive, reducing UTCI by 5–6.6 ℃ and neutralizing albedo-driven MRT increases.

Accordingly, urban design guidelines should prioritize combined strategies that integrate reflective pavements with vertical shading, vegetation, and context-specific morphological adjustments. Future research should extend beyond summer peak simulations to include seasonal variation, façade reflectivity, and long-term monitoring of albedo degradation under dusty climates, ensuring that such passive cooling strategies remain robust and effective in real-world applications.

# 6. Practical and Policy Implications for Urban Planners

The outcomes of this study demonstrate the need for integrated urban cooling strategies in hot-arid environments such as New Cairo, where material interventions alone may exacerbate thermal discomfort. While high-albedo surfaces effectively reduce surface and $T_a$, the concurrent rise in Mean Radiant Temperature (MRT) and Universal Thermal Climate Index (UTCI) highlights the physiological trade-offs of relying solely on reflective materials [3], [5], [9], [47]. Policy guidance should therefore prioritize layered interventions (material reflectance plus geometric shade and greenery) as recommended by recent integrative reviews of city-scale heat mitigation [8].

Urban planning policies should therefore mandate the pairing of reflective surfaces with adequate shading solutions (such as tree canopies, pergolas, and arcades) to counterbalance increased shortwave radiation redirected toward pedestrians [6], [16], [37], [38], with additional consideration of how urban morphology shapes exposure [37].

Given the harsh, dusty climate of many arid cities, including Cairo, it is also essential that planners account for the temporal degradation of albedo due to dust accumulation and wear [15]. To ensure sustained cooling benefits, maintenance protocols (such as scheduled cleaning or selection of high-durability coatings) should be institutionalized in public space management plans.

Furthermore, public outreach initiatives can play a key role in supporting implementation. Educating developers, municipal authorities, and the public on the dual nature of high-albedo materials (both as cooling agents and potential sources of thermal stress) will foster more informed, resilient design decisions. This echoes recommendations of Liu et al. [5] who stressed the importance of stakeholder engagement in microclimatic planning.

In conclusion, this study advocates for a paradigm shift from singular material-based approaches to comprehensive urban heat mitigation frameworks. Effective thermal design in hot-arid environments must consider the interactive roles of albedo, shading, and maintenance, ensuring that pedestrian comfort is enhanced without unintended consequences. Policymakers in rapidly urbanizing districts should prioritize these synergies to build thermally adaptive, climate-resilient cities.

# 7. Research Limitations

This study focused solely on the thermal effects of surface albedo variation under peak summer conditions in a hot-arid climate. While this enabled a controlled evaluation of material reflectivity on pedestrian thermal comfort, several limitations must be acknowledged.

First, the simulations deliberately excluded vegetation, shading devices, and street furniture to isolate the impact of surface albedo. However, in actual urban environments, vegetation plays a vital role in intercepting and absorbing shortwave radiation, thereby moderating the MRT increases typically observed in exposed reflective surfaces. Through canopy coverage and evapotranspiration, vegetation helps reduce thermal stress by capturing a portion of the radiative load and releasing latent heat. These effects were not simulated in this study. As such, the rise in MRT and UTCI values under high-albedo scenarios may be overstated compared to vegetated real-world settings. Consistent with review findings, comfort outcomes remain sensitive to morphology, exposure, and maintenance, limiting direct transferability across typologies without local calibration [8].

Second, the analysis was confined to a single peak summer day (August 15), limiting the generalizability of the findings across seasons or transitional periods such as spring or autumn. Material thermal performance and human comfort thresholds may vary significantly throughout the year.

Finally, the study focused on a single urban typology (a low-rise commercial strip), which limits the applicability of the results to other urban forms such as compact residential blocks or shaded courtyards. In hot-arid Tehran, reorienting buildings yielded the greatest air-temperature reduction (~1.69 ℃), underscoring the role of geometry alongside vegetation and materials [50]. Future research should incorporate diverse urban geometries and landscape elements to better understand the interactive thermal effects of materials and spatial design [50].

# 8. Future Research

Building on the findings of this study, future research should incorporate more holistic simulation scenarios that combine reflective materials with vegetation, shading devices, and varied urban typologies. Future work should reflect review recommendations to test multi-strategy bundles across seasons and to track durability (soiling/aging) to ensure sustained performance of reflective surfaces [8]. In addition, integrating long-term durability factors is essential, since reflective pavements in arid climates can show performance decline under weathering and soiling [4]. Validated workflows, such as Kamel's Egypt-focused parametric simulation framework, demonstrate how durability and climatic factors can be systematically incorporated into long-term comfort modelling [21]. While the present analysis isolated the role of albedo to clarify its individual thermal impact, subsequent investigations should assess the interactive effects of multi-layered design strategies on thermal comfort.

Integrating vegetative elements alongside reflective pavements would provide a more realistic representation of urban microclimates. Vegetation contributes both shading (reducing MRT) and latent cooling through evapotranspiration; mechanisms consistently emphasized in systematic reviews of thermal comfort studies [35]. Additional research is needed to quantify how greenery might offset the intensified shortwave radiation associated with high-albedo materials.

Future simulations should also be extended across multiple seasons to capture thermal performance variations under different climatic conditions. This would increase the relevance of findings for long-term urban planning and design strategies [9].

Another critical direction involves the long-term performance of reflective materials. Albedo degradation due to dust accumulation and surface wear can significantly alter thermal outcomes. Longitudinal studies under real-world arid conditions, such as those in Cairo, are necessary to validate maintenance cycles and inform material selection policies.

Lastly, future research should explore diverse urban configurations (such as compact residential districts, internal courtyards, and transit strips) to better understand how spatial morphology interacts with reflective strategies in regulating pedestrian thermal comfort [38].

# Declaration of Generative AI and AI-Assisted Technologies in the Writing Process

During the preparation of this work, the author(s) used ChatGPT 5/OpenAI in order to improve readability. After using this tool/service, the author(s) reviewed and edited the content as needed and take(s) full responsibility for the content of the publication.

# REFERENCES


[1] Y. Luo *et al.*, “Seasonal cooling effect of vegetation and albedo applied to surface urban heat island (SUHI) mitigation in three Chinese megacities,” *Remote Sensing*, vol. 15, no. 23, p. 5478, 2023, doi: 10.3390/rs15235478.

[2] R. A. Abdelwahab, A. A. Fekry, and R. E.-D. Hamed, “The effective landscape design parameters with high reflective hardscapes: Guidelines for optimizing human thermal comfort in outdoor spaces by design-A case on hot arid climate weather,” Computational Urban Science, vol. 5, no. 1, Article 28, 2025, doi: 10.1007/s43762-025-00186-w.

[3] H. Elmagri, T. Kamel, and H. Ozer, "Assessment of the effectiveness of cool pavements on outdoor thermal environment in urban area," Building and Environment, vol. 266, pp. 112095, 2024, doi: 10.1016/j.buildenv.2024.112095.

[4] F. A. Schneider, J. C. Ortiz, J. K. Vanos, D. J. Sailor, and A. Middel, “Evidence-based guidance on reflective pavement for urban heat mitigation in Arizona,” *Nature Communications*, vol. 14, p. 1467, 2023, doi: 10.1038/s41467-023-36972-5.

[5] Y. Liu, C. Chu, R. Zhang, S. Chen, C. Xu, and D. Zhao, “Impacts of high-albedo urban surfaces on outdoor thermal environment across morphological contexts: A case of Tianjin, China,” Sustainable Cities and Society, vol. 100, pp. 105038, 2024, doi: 10.1016/j.scs.2023.105038.

[6] D. Elgendy, O. Tolba, and T. Kamel, “The impact of increasing urban surface albedo on outdoor air and surface temperatures during summer in newly developed areas,” *Scientific Reports*, vol. 15, no. 1, p. 25874, 2025, doi: 10.1038/s41598-025-08574-2.

[7] T. M. Kamel, R. Khalil, M. Hamdy, A. Khalil, and M. M. Lakousha, “Assessment of land cover strategies for lowering outdoor air temperatures and cooling resilience in partially air-conditioned buildings in hot-arid urban areas,” *Sustainable Cities and Society*, vol. 131, p. 106762, 2025, doi: 10.1016/j.scs.2025.106762.

[8] S. Tsoka, K. Tsikaloudaki, T. Theodosiou, and D. Bikas, “Urban Warming and Cities’ Microclimates: Investigation Methods and Mitigation Strategies—A Review,” Energies, vol. 13, no. 6, Art. no. 1414, Mar. 2020, doi: 10.3390/en13061414.

[9] R. Aghamolaei, M. Taleghani, and M. Tenpierik, “A comprehensive review of outdoor thermal comfort in urban areas: Geometry and layout focused,” *Energy and Buildings*, vol. 290, p. 113047, 2023, doi: 10.1177/0958305X221116176.

[10] B. Bedra and D. Li, “Relevance of ground and wall albedo for outdoor thermal comfort in tropical savanna climates: Parametric ENVI-met simulations,” *Sustainability*, vol. 17, no. 14, p. 6303, 2025, doi: 10.3390/su17146303.

[11] C. K. C. Lam, J. Weng, K. Liu, and J. Hang, “The effects of shading devices on outdoor thermal and visual comfort in Southern China during summer,” *Building and Environment*, vol. 228, Art. 109743, 2023, doi: 10.1016/j.buildenv.2022.109743.

[12] I. Kousis and A. L. Pisello, “Evaluating the performance of cool pavements for urban heat island mitigation under realistic conditions: A systematic review and meta-analysis,” *Urban Climate*, vol. 49, p. 101470, 2023, doi: 10.1016/j.uclim.2023.101470.

[13] S. Kappou, M. Souliotis, S. Papaefthimiou, and M. Santamouris, “Cool pavements: State of the art and new technologies,” *Sustainability*, vol. 14, no. 9, p. 5159, May 2022, doi: 10.3390/su14095159.

[14] R. Soares, H. Corvacho, and F. Alves, “Summer thermal conditions in outdoor public spaces: A case study in a Mediterranean climate,” *Sustainability*, vol. 13, no. 10, p.

5348, 2021, doi: 10.3390/su13105348.

[15] H. Ashraf, T. A. El Seoud, S. Sodoudi, and A. El-Zafarany, “Anisotropic surface urban heat island in Cairo: Spatiotemporal thermal comfort responses,” *Civil Engineering and Architecture*, vol. 11, no. 1, pp. 331–350, 2023, doi: 10.13189/cea.2023.110127.

[16] G. Del Serrone, P. Peluso, and L. Moretti, “Evaluation of microclimate benefits due to cool pavements and green infrastructures on urban heat islands,” *Atmosphere*, vol. 13, no. 10, p. 1586, 2022, doi: 10.3390/atmos13101586.

[17] K. Li, Y. Zhao, J. Liu, and H. Zhang, “Evaluating the performance of different thermal indices on outdoor thermal comfort in humid subtropical residential areas of China,” *Frontiers in Environmental Science*, vol. 10, art. 1071668, 2022, doi: 10.3389/fenvs.2022.1071668.

[18] M. Mahdavinejad, S. Parsaee, H. Dehghani, and M. Mohammadi, “Comparing Universal Thermal Climate Index (UTCI) with selected thermal indices to evaluate outdoor thermal comfort in traditional courtyards with BWh climate,” *Sustainable Cities and Society*, vol. 110, p. 105229, 2024, doi: 10.1016/j.uclim.2024.101839.

[19] R. N. Faragallah and R. A. Ragheb, “Evaluation of thermal comfort and urban heat island through cool paving materials using ENVI-Met,” Ain Shams Engineering Journal, vol. 13, no. 4, p. 101609, 2022, doi: 10.1016/j.asej.2021.10.004.

[20] T. Roba, B. Fekadu, and Y. Tadesse, “Geospatial analysis of vegetation impact on land surface temperature in Addis Ababa,” *Scientific Reports*, vol. 15, no. 17014, 2025, doi: 10.1038/s41598-025-17014-0.

[21] T. M. Kamel, “A new comprehensive workflow for modelling outdoor thermal comfort in Egypt,” Solar Energy, vol. 225, pp. 162–172, 2021, doi: 10.1016/j.solener.2021.07.029.

[22] Y. I. Ibrahim, T. Kershaw, and P. Shepherd, “Improvement of the Ladybug-tools microclimate workflow: A verification study,” in *Proceedings of the IBPSA-England Building Simulation and Optimisation Conference*, Loughborough, U.K., Sep. 2020. [Online]. Available: https://www.researchportal.bath.ac.uk/files/212194313/Improvement_of_the_Ladybug_tools_microclimate_workflow_A_verification_study.pdf.

[23] C. Ghenai, O. Rejeb, T. Sinclair, N. Almarzouqi, N. Alhanaee, and F. Rossi, “Evaluation and thermal performance of cool pavement under desert weather conditions: Surface albedo enhancement and carbon emissions offset,” Case Studies in Construction Materials, vol. 18, p. e01940, Jul. 2023, doi: 10.1016/j.cscm.2023.e01940.

[24] M. Abd Elraouf, S. Attia, and M. Shafiekhani, “Evaluating urban outdoor thermal comfort: Validation of ENVI-met simulation through field measurement,” Journal of Building Performance Simulation, vol. 15, no. 2, pp. 268–286, 2022, doi: 10.1080/19401493.2022.2046165.

[25] A. Ferrari, A. Kubilay, D. Derome, and J. Carmeliet, “The use of permeable and reflective pavements as a potential strategy for urban heat island mitigation,” Urban Climate, vol. 31, 100534, 2020, doi: 10.1016/j.uclim.2019.100534.

[26] P. Mohammad, S. Aghlmand, A. Fadaei, S. Gachkar, D. Gachkar, and A. Karimi, “Evaluating the role of the albedo of material and vegetation scenarios along the urban street canyon for improving pedestrian thermal comfort outdoors,” Urban Climate, vol. 40, p. 100993, 2021, doi: 10.1016/j.uclim.2021.100993.

[27] P. J. Crank, A. Middel, M. Wagner, D. Hoots, M. Smith, and A. Brazel, “Validation of seasonal mean radiant temperature simulations in hot arid urban climates,” *Science of the Total Environment*, vol. 749, p. 141392, 2020, doi: 10.1016/j.scitotenv.2020.141392.

[28] O. Aleksandrowicz, T. Saroglou, and D. Pearlmutter, “Evaluation of summer mean radiant temperature simulation in ENVI-met in a hot Mediterranean climate,” *Building and Environment*, vol. 245, Art. no. 110881, Nov. 2023, doi: 10.1016/j.buildenv.2023.110881.

[29] International Organization for Standardization, *ISO 7726: Ergonomics of the Thermal Environment – Instruments for Measuring Physical Quantities*, Geneva, Switzerland: ISO, 1998 (confirmed 2024). [Online]. Available: https://www.iso.org/standard/14562.html.

[30] Anand, J., and D. J. Sailor, “Role of pavement radiative and thermal properties in reducing excess heat in cities,” *Solar Energy*, vol. 242, pp. 413–423, 2022, doi: 10.1016/j.solener.2021.10.056.

[31] I. Elwy, Y. Ibrahim, M. Fahmy, and M. Mahdy, “Outdoor microclimatic validation for hybrid simulation workflow in hot arid climates against ENVI-met and field measurements,” *Energy Procedia*, vol. 153, pp. 29–34, 2018, doi: 10.1016/j.egypro.2018.10.009.

[32] X. Zhou, Y. Sun, T. Li, Y. Zhou, T. Tan, C. Yu, and S. Dai, “Optimizing Microclimate Comfort in Macao: ENVI-Met Simulation of High-Density Urban Layouts Under the Climate in the Lingnan Area,” *Atmosphere*, vol. 16, no. 1, p. 70, 2025, doi: 10.3390/atmos16010070.

[33] H. Alsaad, “ENVI-met validation data accompanied with simulation data for microclimate and thermal comfort research,” *Data in Brief*, vol. 41, p. 107968, 2022, doi: 10.1016/j.dib.2022.108200.

[34] A. Salvati, A. Coch Roura, C. Cecere, F. Cotana, R. De Lieto Vollaro, C. Piselli, M. Pisello, and M. Santamouris, “Impact of reflective materials on urban canyon albedo, outdoor and indoor microclimates,” *Building and Environment*, vol. 207, p. 108459, 2022, doi: 10.1016/j.buildenv.2021.108459.

[35] Mandić, L., Đjukić, A., Marić, J., Mitrović, B., “A Systematic Review of Outdoor Thermal Comfort Studies for the Urban (Re)Design of City Squares,” Sustainability, vol. 16, no. 12, p. 4920, 2024, doi: 10.3390/su16124920.

[36] M. E. El-Bahrawy, “Investigating Ladybug as a Tool for Measuring Outdoor Thermal Comfort in Urban Neighborhoods,” Alexandria Engineering Journal, vol. 63, no. 12, pp. 1127–1139, 2024, doi: 10.21608/jesaun.2023.234735.1256.

[37] K. B. Bedra, “Evaluation of outdoor thermal comfort under different urban morphology scenarios using ENVI-met simulations in a tropical savanna climate,” *Sustainability*, vol. 15, no. 11, p. 8902, 2023, doi: 10.3390/su15118902.

[38] Q. Zhang, X. Ma, D. Xu, D. Zhou, Y. Yang, and W. Jiang,

"The Impact of Courtyard Spatial Characteristics Across Historical Periods on Summer Microclimates: A Case Study from China," *Buildings*, vol. 15, no. 2, art. 224, 2025, doi: 10.3390/buildings15020224.

[39] F. M. Alves, "The Use of Envi-Met for the Assessment of Nature-Based Solutions: Diurnal Variation of Mean Radiant Temperature in Urban Public Spaces," *Infrastructures*, vol. 7, no. 6, p. 85, 2022, doi: 10.3390/infrastructures7060085.

[40] F. Hashemi, U. Poerschke, L. D. Iulo, and G. Chi, "Urban microclimate, outdoor thermal comfort, and socio-economic mapping: A case study of Philadelphia, PA," *Buildings*, vol. 13, no. 10, p. 1040, 2023, doi: 10.3390/buildings13041040.

[41] A. Alzahrani and M. Gadi, "Assessment of Modeled Mean Radiant Temperature in Hot and Dry Environments: A Case Study in Saudi Arabia," *Climate*, vol. 12, no. 7, p. 91, 2024, doi: 10.3390/cli12070091.

[42] JJ. Wu, H. Chang, and S. Yoon, "Numerical Study on Microclimate and Outdoor Thermal Comfort of Street Canyon Typology in Extremely Hot Weather - A Case Study of Busan, South Korea," *Atmosphere*, vol. 13, no. 2, p. 307, 2022, doi: 10.3390/atmos13020307.

[43] Y. I. Ibrahim, F. Tabish, and J. Owen, "Improvement of the Ladybug Tools microclimate workflow: A verification study," Univ. of Bath Research Repository, Bath, U.K., 2021. [Online]. Available: https://researchportal.bath.ac.uk/en/publications/improvement-of-the-ladybug-tools-microclimate-workflow-a-verifica.

[44] W. Ouyang, T. Sinsel, H. Simon, T.E. Morakinyo, H. Liu, and E. Ng, "Evaluating the thermal-radiative performance of ENVI-met model for green infrastructure typologies: Experience from a subtropical climate," *Building and Environment*, vol. 207, p. 108427, 2022, doi: 10.1016/j.buildenv.2021.108427.

[45] A. Aboelata, "Reducing outdoor air temperature, improving thermal comfort, and saving buildings' cooling energy demand in arid cities-Cool paving utilization," *Sustainable Cities and Society*, vol. 68, p. 102762, 2021, doi: 10.1016/j.scs.2021.102762.

[46] V. P. López-Cabeza, S. Alzate-Gaviria, E. Diz-Mellado, C. Rivera-Gomez, and C. Galan-Marin, "Albedo influence on the microclimate and thermal comfort of courtyards under Mediterranean hot summer climate conditions," *Sustainable Cities and Society*, vol. 81, p. 103872, 2022, doi: 10.1016/j.scs.2022.103872.

[47] C. Di Napoli, A. Messeri, M. Novák, J. Rio, J. Wieczorek, M. Morabito, P. Silva, A. Crisci, and F. Pappenberger, "The universal thermal climate index as an operational forecasting tool of human biometeorological conditions in Europe," in *Applications of the Universal Thermal Climate Index (UTCI) in Biometeorology*, E. L. Krüger, Ed., Cham: Springer, 2021, pp. 193–208, doi: 10.1007/978-3-030-76716-7_10.

[48] S. Shooshtarian, C. K. C. Lam, and I. Kenawy, "Outdoor thermal comfort assessment: A review on thermal comfort research in Australia," *Building and Environment*, vol. 177, art. 106917, 2020, doi: 10.1016/j.buildenv.2020.106917.

[49] L. Chen, Y. Zhang, J. Han, and X. Li, "An investigation of the influence of ground surface properties and shading on outdoor thermal comfort in a high-altitude residential area," *Frontiers of Architectural Research*, vol. 10, no. 2, pp. 432–446, 2021, doi: 10.1016/j.foar.2020.12.005.

[50] H. Farhadi, M. Faizi, and H. Sanaieian, "Mitigating the urban heat island in a residential area in Tehran: Investigating the role of vegetation, materials, and orientation of buildings," *Sustainable Cities and Society*, vol. 46, p. 101448, 2019, doi: 10.1016/j.scs.2019.101448.

[51] H. Necira, M. E. Matallah, S. Bouzaher, W. A. Mahar, and A. Ahriz, "Effect of Street Asymmetry, Albedo, and Shading on Pedestrian Outdoor Thermal Comfort in Hot Desert Climates," *Sustainability*, vol. 16, no. 3, Art. 1291, 2024, doi: 10.3390/su16031291.

[52] S. Croce, A. Lucchese, G. Pellizzari, and S. Carlucci, "The Use of Cool Pavements for the Regeneration of Industrial Areas: A Microclimate Analysis," *Sustainability*, vol. 13, no. 11, Art. 6322, 2021, doi: 10.3390/su13116322.